JBC Papers in Press. Published on February 3, 2017 as Manuscript M116.774448
The latest version is at http://www.jbc.org/cgi/doi/10.1074/jbc.M116.774448

Kinetic Mechanism of the Dechlorinating Flavin-Dependent Monooxygenase HadA

Panu Pimviriyakul[1], Kittisak Thotsaporn[2], Jeerus Sucharitakul[2] and Pimchai Chaiyen[1]*

[1]Department of Biochemistry and Center for Excellence in Protein and Enzyme Technology, Faculty of Science, Mahidol University, Bangkok, Thailand 10400.
[2]Department of Biochemistry, Faculty of Dentistry, Chulalongkorn University, Bangkok, Thailand 10300.

*Running title: *Kinetic Mechanism of HadA monooxygenase*

*Corresponding authors
E-mail: pimchai.cha@mahidol.ac.th. Phone: +66-2201 5596. Fax: +66-2354 7174.

Keywords: flavin-dependent monooxygenase, transient kinetics, oxygenase, dechlorinase, chlorophenols (CPs).

ABSTRACT

The accumulation of chlorophenols (CPs) in the environment, due to their wide use as agrochemicals, has become a serious environmental problem. These organic halides can be degraded by aerobic microorganisms, where the initial steps of various biodegradation pathways include an oxidative dechlorinating process in which chloride is replaced by a hydroxyl substituent. Harnessing these dechlorinating processes could provide an opportunity for environmental remediation, but detailed catalytic mechanisms for these enzymes are not yet known. To close this gap, we now report transient kinetics and product analysis of the dechlorinating flavin-dependent monooxygenase, HadA, from the aerobic organism *Ralstonia pickettii* DTP0602, identifying several mechanistic properties that differ from other enzymes in the same class. We first overexpressed and purified HadA to homogeneity. Analyses of the products from single and multiple turnover reactions demonstrated that HadA prefers 4-CP and 2-CP over CPs with multiple substituents. Stopped-flow and rapid-quench flow experiments of HadA with 4-CP show the involvement of specific intermediates (C4a-hydroperoxy-FAD and C4a-hydroxy-FAD) in the reaction, define rate constants and the order of substrate binding, and demonstrate that the hydroxylation step occurs prior to chloride elimination. The data also identify the non-productive and productive paths of the HadA reactions and demonstrate that product formation is the rate-limiting step. This is the first elucidation of the kinetic mechanism of a two-component flavin-dependent monooxygenase that can catalyze oxidative dechlorination of various CPs, and as such will serve as the basis for future investigation of enzyme variants that will be useful for applications in detoxifying chemicals hazardous to human health.

Chlorophenols (CPs) such as 2,4,6-trichlorophenol (2,4,6-TCP), 2,4-dichlorophenol (2,4-DCP) and pentachlorophenol (PCP) are commonly used as herbicides, insecticides and fungicides in agricultural industries. CPs can also be derived from pesticide degradation. For example, 2,4,5-trichlorophenol (2,4,5-TCP) is derived from the degradation of 2,4,5-trichlorophenoxyacetate (1), and 2-chloro-4-bromo phenol is derived from the organophosphate insecticide, profenofos (2). These compounds are classified as persistent environmental pollutants that can accumulate in water and soil (3), and most of them are registered under the priority pollutants list (4) and/or the priority list of hazardous substances (5). High human exposure to these compounds can lead to severe health problems such as cancer, DNA damage, organ damage, or even acute death (3,6-8). As these compounds are found widespread in the environment due to their utilization in agriculture and in industrial processes, a biodegradation process that can provide a sustainable method to detoxify them is essential to the reduction of CP contamination in fresh water and soil.

Many aerobic biological systems have shown promising activity in degrading CPs. Degradation of CPs such as 2,4,5-TCP, 2,4,6-TCP, or PCP can be carried out by various enzymatic systems such as *tft* clusters from *Burkholderia cepacia* AC1100 (9,10), *tcp* clusters from *Ralstonia eutropha* JMP134 (11-13), *had* clusters from *Ralstonia pickettii* DTP0602 (14-16) and *pcp* clusters from *Sphingobium chlorophenolicum* (17-19).

Aerobic biodegradation of CPs generally involves replacement of a chloride group by a hydroxyl group in the initial steps of these biodegradation pathways. This oxidative dehalogenation is often catalyzed by flavin-dependent monooxygenases (20). These oxygenases include both types of monooxygenases-those that utilize a single protein, as well as those that utilize two proteins. The most well studied single-component flavin-dependent dechlorinase is PcpB from *S. chlorophenolicum*. This enzyme binds to FAD as a cofactor and requires NADPH and O_2 as co-substrates for the conversion of PCP to 2,3,5,6-tetrachlorobenzoquinone (2,3,5,6-TCBQ) in the initial step of PCP degradation. The quinone product can be chemically reduced to 2,3,5,6-tetrachloro-*p*-hydoquinone (2,3,5,6-TCHQ) (18,19). However, turnover of PcpB using PCP as a substrate is very slow, implying that PCP may not be a native substrate of PcpB (18). Many oxidative dechlorination reactions are also catalyzed by two-component flavin-dependent enzymes including TftD from *B. cepacia* AC1100 (9,10), TcpA from *R. eutropha* JMP134 (13), and HadA from *R. pickettii* DTP0602 (15). Although a few of these enzymes have been shown to catalyze oxidative dechlorination of CPs, their reaction mechanisms are not well understood. None of these enzymes have been explored with regards to their kinetic mechanisms, and the rate constants associated with the individual steps have yet to be measured. Only X-ray structures of TftD and TcpA and the overall bioconversion activities of these enzymes have been reported (9,10,13,15,21).

Based on previous reports, the substrate utilization of HadA (14,15) seems to be broader than that of TcpA (specific to 2,4,6-TCP; 86.7% identity to HadA) and TftD (specific for 2,4,5-TCP; 64.2% identity to HadA), making HadA attractive for development as a biocatalyst for CP detoxification. Previously, studies of the HadA reaction were only carried out with whole cells and lysates of cells overexpressing HadA (14,15) without measuring the products that were specifically generated from the flavin-bound enzyme. As study of the transient kinetics of a two-component flavin-dependent dechlorinase has not been reported, we have chosen HadA as a model for investigating the substrate utilization and rate constants associated with the individual steps under single turnover conditions to identify the flavin species and reaction steps and pathways involved in oxidative dechlorination.

Based on sequence similarity, HadA belongs to the family of two-component flavin-dependent monooxygenases that utilize two separate proteins in their catalysis (Class D monooxygenase) (22). A reductase component of these enzymes catalyzes flavin reduction, while an oxygenase component catalyzes substrate oxygenation (22,23). The most well-studied enzyme in this family is *p*-hydroxyphenylacetate hydroxylase (HPAH) from *Acinetobacter baumannii*. The mechanism of reduced flavin generation by the reductase (C_1), as well as the mechanism of the oxygenase (C_2) reaction, have been determined for this enzyme. Furthermore, the individual rate constants associated with each step and the mechanism of reduced flavin transfer between the two components have been reported (24-30). This knowledge has been useful for applying HPAH for the synthesis of bioactive phenolic acids and in the hydroxylation of aniline derivatives (31,32).

When the sequence of HadA was examined by sequence similarity network (SSN) analysis using the Enzyme Function Initiative (EFI) program to determine its relationship with any homologous enzymes known to date, the results (Fig. S1) showed that there are 2,839 enzymes in which the sequences have >34% identity with HadA and only 11 out of these 2,839 enzymes were reviewed by UniProt. The enzymes identified to be homologous to HadA were mostly flavin-dependent monooxygenases that incorporate a hydroxyl group into phenols such as CPs or nitrophenols (9,10,33-35). As these enzymes showed potential applications in bioremediation of toxic compounds, the understanding of kinetic mechanisms associated with a flavin-dependent

dechlorinase (HadA) reported herein should also be useful for giving an overall picture about the reaction mechanism of these enzymes in general.

In this work, the enzyme from *R. pickettii* DTP0602 (HadA) was overexpressed, purified to homogeneity, and its reaction with several CPs were explored. The reactions of HadA with 4-chlorophenol (4-CP, the most optimal substrate) were investigated using stopped-flow and rapid quench-flow techniques to measure the rate constants associated with the individual steps. The results clearly determined the order of substrate binding and the rate constants associated with each of the individual steps, and identified C4a-hydroperoxy-FAD and C4a-hydroxy-FAD as intermediates in the dechlorination process catalyzed by HadA.

RESULTS

Expression and purification of HadA. Recombinant HadA was overexpressed and purified according to the purification methods described in the *Experimental Procedures* to yield protein with >95% purity (Fig. S2). The protein preparation protocol resulted in ~0.6 g of purified HadA from 3.9 l of culture. HadA had no cofactor bound and the native molecular mass suggests that HadA is a tetrameric protein with a subunit molecular mass of ~59 kDa (Fig. S3).

Flavin specificity of HadA. As HadA is the oxygenase component of a two-component flavin-dependent monooxygenase, we first needed to identify its flavin specificity and its ability to form C4a-hydroperoxyflavin. The enzymes in this class use specific reduced flavins as substrates and form C4a-hydroperoxyflavin as a reactive intermediate to perform monooxygenation plus other additional activities (22,23,36,37). Binding of $FADH^-$ or $FMNH^-$ to HadA was investigated to identify which flavin could bind to HadA and yield a binary complex able to react with oxygen. Solutions of $FADH^-$ and $FMNH^-$ were mixed with buffers containing oxygen (air saturation) in the presence or absence of HadA. The results indicate that only the oxidation of $FADH^-$ was affected by the presence of HadA, indicating that the enzyme can only bind to $FADH^-$ and not $FMNH^-$ (Fig. S4). The reaction of free $FADH^-$ with oxygen showed an increase in absorbance at 380 and 450 nm with an observed rate constant of ~2.3 s^{-1} (red lines, Fig. S4A). In the presence of HadA, the oxidation of $FADH^-$ resulted in two observable phases. The first phase consisted of a large absorbance increase at 380 nm (blue solid line, Fig. S4A), while the second phase was characterized by a large and slow (observed rate constant of 0.005 s^{-1}) increase in absorbance at 450 nm (blue dashed line, Fig. S4A). These data indicate that in the presence of HadA, $FADH^-$ oxidation resulted in the formation of C4a-hydroperoxy-FAD which can be detected by a large absorbance increase at 380 nm where C4a-hydroperoxy-FAD absorbs maximally (more analysis to follow). The mixing of $FMNH^-$ with air-saturated HadA (blue lines, Fig. S4B) yielded the same kinetic traces as those of the reaction without HadA (red lines, Fig. S4B). Both reactions showed the increase in absorbance at 380 and 446 nm with an observed rate constant of 3.2 s^{-1}. These data clearly suggest that HadA can only bind to $FADH^-$ and not $FMNH^-$.

Identification of product from HadA single turnover reactions. In order to identify the substrate specificity of HadA, the products resulting from single turnover reactions of HadA (see *Experimental Procedures*) were identified by comparing their HPLC and mass spectroscopic profiles with those of standard compounds. As most of the products were expected to be quinone derivatives, ascorbic acid (1 mM) was added into the reaction to convert them into their hydroquinone form which is more stable. The results of the product identification studies (Table 1, Figs. S5A-S5C) show that HadA catalyzes the hydroxylation of various CPs including 4-chlorophenol (4-CP), 2-chlorophenol (2-CP), 2,4-dichlorophenol (2,4-DCP), 2,4,5-trichlorophenol (2,4,5-TCP) and 2,4,6-trichlorophenol (2,4,6-TCP) to produce hydroquinone (HQ), chlorohydroquinone (CHQ), 2,5-dichlorohydroquinone (2,5-DCHQ), and 2,6-dichlorohydroquinone (2,6-DCHQ), respectively. The product identification results are summarized in Table 1. Based on these reactions, HadA incorporates a hydroxyl group at the *para*-position of the original hydroxyl group of all five substrates investigated. When the *para*-position contains a chloride substituent (in the case of 4-CP, 2,4-DCP, 2,4,5-TCP and 2,4,6-TCP), HadA catalyzes hydroxylation plus Cl^- elimination (Fig. 1). Comparison of the percentage of product formation

after single turnover reactions for the different substrates indicates that HadA prefers to use mono-substituted CPs over multiple-substituted CPs. These results contradict previously reported data from cell lysate experiments (where HadA was not purified) in which 2,4,6-TCP was reported as the most preferred substrate for HadA (14,15).

Comparison of multiple turnover reactions of HadA with various chlorophenols. As the results from the single turnover experiments in Table 1 are different from those previously reported (14,15), multiple turnover reactions of HadA (see *Experimental Procedures*) with various substrates were carried out to identify which compounds among 4-CP, 2,4-DCP, 2,4,5-TCP, and 2,4,6-TCP, are the preferred substrates for the HadA bioconversion process. The results (Fig. 2) show that under the same experimental conditions, 4-CP, 2,4-DCP, and 2,4,5-TCP were completely converted to HQ, CHQ, and 2,5-DCHQ with half-times ($t_{1/2}$) of the reactions around 13, 35, 56 min, respectively (Figs. 2A-C). In contrast, 2,4,6-TCP was only 72% depleted after 600 min (Fig. 2D). These data agree with the results from single turnover reactions (Table 1) which indicated that the efficiency of HadA hydroxylation of 4-CP (49%) is greater than that of 2,4-DCP (14%), 2,4,5-TCP (9%), and 2,4,6-TCP (4%).

Preference of hydroxylation site identified by multiple turnover reactions of HadA and 2,4,5-TCP. The results in Fig. 2C also show that the product from 2,4,5-TCP multiple turnover reactions, 2,5-DCHQ, decreased over time, indicating that the compound may be further hydroxylated. To characterize the nature of the second conversion step of 2,4,5-TCP, the reaction of HadA with 2,5-DCHQ was investigated. The results showed that 2,5-DCHQ was completely depleted within 4 hrs (Fig. S6A), with concomitant appearance of a hydroxylation product which has an *m/z* of +16 atomic units compared to the value for 2,5-DCHQ. This compound also has mass spectroscopic and HPLC profiles consistent with those of 5-chlorohydroxyquinol (5-CHQL) **(**Figs. S6A-B). All results suggest that HadA can convert 2,5-DCHQ to 5-CHQL**.** Therefore, the overall reaction of HadA and 2,4,5-TCP can be summarized as in Fig. 3 in which the first hydroxylation and Cl^- elimination step occurs at position 4 and then the second hydroxylation and Cl^- elimination step proceeds at position 2.

pH optimization of HadA. In order to identify the optimum pH for the HadA reaction to be used in transient kinetics experiments, single turnover reactions of HadA and its best substrate, 4-CP were carried out at various pHs and the amount of product formation was analyzed according to the protocol described in the *Experimental Procedures*. An anaerobic solution of HadA:$FADH^-$ in 20 mM HEPES pH 7.5 was mixed with an equal volume of an aerobic solution of 4-CP at various pH values from 6.5-10.5. The HQ production results (Fig. 4) indicated that the reaction of HadA has an optimum pH within the range of ~7.0-8.2. Therefore, the transient kinetics experiments were all performed at pH 7.5. (Transient kinetic experiments were also performed at various pHs to explore if pH affects the ability of HadA to form C4a-hydroperoxy-FAD (shown in Section. F).

Effect of ascorbic acid on the HadA reaction. As most of the reactions in this report contained ascorbic acid (1 mM) to stabilize the hydroquinone products, the effect of ascorbic acid on the reaction of HadA was investigated. The transient kinetics of the HadA reactions in the absence or presence of ascorbic acid was investigated using stopped-flow techniques. A solution of the HadA:$FADH^-$ binary complex was mixed with air-saturated 20 mM HEPES pH 7.5 in the presence or absence of 1 mM ascorbic acid on the stopped-flow spectrophotometer. Kinetic traces of both experiments were almost identical (Fig. S7), suggesting that ascorbic acid does not interfere with HadA catalytic behavior and that it can be used for stabilizing the substrate and product in the HadA reaction.

Reaction mechanism of HadA with 4-CP as a substrate investigated by transient kinetics.

A. Binding of $FADH^-$. (Step 1 in Fig. 5; $FADH^-$ is the first substrate to bind to HadA)

For two-component flavin-dependent monooxygenases that use reduced flavin as a substrate such as HadA, the enzyme must bind to $FADH^-$ to form an active binary complex HadA:$FADH^-$ before it can react with oxygen to form C4a-hydroperoxy-FAD.

A.1. Dissociation constant (K_d) of binding of HadA and FADH$^-$.

The K_d for the binding of HadA and FADH$^-$ can be measured based on the amount of the binary complex formed which can further react with oxygen to form C4a-hydroperoxy-FAD (Fig. S4). A solution of anaerobic FADH$^-$ (12.5 μM) was mixed with air saturated HadA (0-0.4 mM) in the stopped-flow apparatus. The concentrations indicated are final concentrations after mixing. The formation of the HadA:FADH$^-$ binary complex is reflected by a slower rate of flavin oxidation (which occurs upon H_2O_2 elimination from C4a-hydroperoxy-FAD, Fig. S4A; Step 8 in Fig. 5) with a $t_{1/2}$ ~100 s (solid lines, Fig. 6). This is much slower than the oxidation rate of free FADH$^-$ ($t_{1/2}$ ~ 0.3 s, dashed line in Fig. 6). When the binding of HadA and FADH$^-$ was not complete, the traces showed two observable phases that directly reflected the oxidation of two distinct species of free and HadA-bound FADH$^-$ (Fig. 6). Therefore, at t=2s, the difference between the absorbance at 450 nm of free FADH$^-$ and that of the HadA-bound FADH$^-$ oxidation represents the amount of HadA:FADH$^-$ binary complex formed. A plot of these values *versus* free HadA concentration represents a binding isotherm that is consistent with the K_d value of 2.0 ± 0.2 μM (*inset* on Fig. 6). This result also established the experimental conditions required to achieve complete binding of FADH$^-$ by HadA (a ratio of HadA:FADH$^-$ as 3:1).

A.2 Kinetics of HadA and FADH$^-$ binding. (Step 1 in Fig. 5)

The binding rate of FADH$^-$ to HadA was measured using double-mixing stopped-flow experiments by monitoring the progress of HadA:FADH$^-$ formation. An anaerobic solution of FADH$^-$ (25 μM) was mixed with an anaerobic solution of HadA (75 μM) in the first mixing step and incubated for various periods of time (0.01-200 s) before oxygenated buffer (air saturation) was added in the second mixing step. Kinetic traces were obtained by monitoring the change of absorbance at 450 nm. A longer preincubation time prior to adding the oxygenated buffer resulted in slower kinetics of absorbance 450 nm increase, raising the $t_{1/2}$ from ~0.3 s (free FADH$^-$ oxidation) to ~100 s (HadA-bound FADH$^-$ reaction). This is because formation of the HadA:FADH$^-$ complex is more complete (as explained above, the HadA:FADH$^-$ binary complex results in formation of C4a-hydroperoxy-FAD which eliminates H_2O_2 slower than the oxidation of free FADH$^-$ (Section A.1)). Results (Fig. S8A) showed that the behavior of free FADH$^-$ oxidation only disappeared when the incubation time of the first mixing was longer than 20 s. A plot of the absorbance changes at 450 nm at 2 s (representing the amount of HadA:FADH$^-$ binary complex formed) *versus* the incubation age time was analyzed according to a single exponential equation to yield an observed rate constant of 0.33 ± 0.04 s^{-1} which is equivalent to a bimolecular rate constant for the binding of HadA and FADH$^-$ of 4.4 ± 0.5 × 10^3 $M^{-1}.s^{-1}$ (*inset* in Fig. S8A).

B: Formation of C4a-hydroperoxyflavin in the HadA reaction.

B.1. Nature of C4a-hydroperoxy-FAD formation. (Step 3 in Fig. 5)

To obtain a spectrum of C4a-hydroperoxy-FAD and to characterize the kinetics of the reaction, a solution of the HadA:FADH$^-$ binary complex was mixed with various concentrations of oxygen in 20 mM HEPES pH 7.5. Analysis of the results (*upper inset* in Fig. 7) indicates that kinetics of these reactions are composed of three phases. The first (0.01-0.2 s) and second (0.2-6 s) phases showed large increases in the absorbance at 380 nm without significant changes at 450 nm. Both phases were dependent on the oxygen concentration. Plots of the observed rate constants (k_{obs}) of both phases *versus* oxygen concentrations were linear, consistent with second-order rate constants of 6.4 ± 0.4 × 10^4 $M^{-1}.s^{-1}$ and 3.3 ± 0.5 × 10^3 $M^{-1}.s^{-1}$ (*lower inset* in Fig. 7), respectively. The dependence of both phases on oxygen concentration suggests that the HadA:FADH$^-$ complex probably exists as a mixture of fast and slow reacting species (Step 2 in Fig. 5). These two phases represent the reaction of the HadA:FADH$^-$ complex with oxygen to form C4a-hydroperoxy-FAD because the spectrum at the end of each phase (solid line with filled circles in Fig. 7) is similar to the spectrum of C4a-hydroperoxyflavin that is produced in the reactions of the oxygenase component of *p*-hydroxyphenylacetate hydroxylase (25) and luciferase (38). The last phase showed a decrease in absorbance at 380 nm and a large increase in absorbance at 450 nm. The observed rate constant was independent of oxygen concentration. This phase represents a slow intermediate decay by H_2O_2

elimination with a rate constant of $5.4 \pm 0.2 \times 10^{-3}$ s^{-1} to form the final species, oxidized FAD (Step 8 in Fig. 5). These data indicate that in the absence of an aromatic substrate, the overall reaction of the binary complex of HadA:$FADH^-$ with oxygen can be summarized as in Steps 3 and 8 in Fig. 5.

B.2. Rate of a conformational change between two forms of the HadA:$FADH^-$ binary complex. (Step 2 in Fig. 5)

We noted that a mixing of an aerobic HadA solution with an anaerobic $FADH^-$ solution resulted in C4a-hydroperoxy-FAD formation with a monophasic kinetic trace (Fig. S4A) which is different from the results in the *upper inset* of Fig. 7 that shows biphasic formation of C4a-hydroperoxy-FAD. These results suggest that pre-incubation of HadA and $FADH^-$ may lead to a conformational change in the enzyme, in which one form of the HadA:$FADH^-$ complex reacts faster with oxygen than the other. To determine whether the pre-incubation of HadA with $FADH^-$ did indeed cause this effect, double-mixing stopped-flow experiments similar to those in Section A.2 were carried out in which the incubation time of the first mixing step to form the HadA:$FADH^-$ complex was varied. In the second mixing step, an oxygenated solution was added to form C4a-hydroperoxy-FAD, which could then be detected at 380 nm (Fig. S8B). The results in Fig. S8B indicate that at an incubation time of <20 s, the kinetics of C4a-hydroperoxy-FAD formation was monophasic with a bimolecular constant of $9.9 \pm 0.1 \times 10^4$ $M^{-1}.s^{-1}$. When the incubation time was increased to greater than 20 s, biphasic kinetics of C4a-hydroperoxy-FAD formation was observed. These results indicate that the biphasic kinetics observed when mixing a preformed binary complex of HadA:$FADH^-$ with oxygen was indeed due to a conformational change in the enzyme to result in two forms of the complex, HadA:$FADH^-$ (fast reacting species) and HadA*:$FADH^-$ (slow reacting species). The rate constant for this enzymatic conformational change was calculated from a plot of ΔA380 nm at t=2 s (the decrease in absorbance at 380 represents conversion of the enzyme to the slow reacting species) *versus* the incubation time as 0.14 ± 0.01 s^{-1} (*inset* in Fig. S8B).

C. Binding of 4-CP and HadA. (Step 10 in Fig. 5, 4-CP can bind to HadA but does not lead to a productive path.)

C.1. 4-CP can also bind to apoHadA and this binding prevents the binding of $FADH^-$.

Although formation of the HadA:$FADH^-$ binary complex in a two-component flavin-dependent monooxygenase is required before the enzyme can react with oxygen, it is known that certain substrates can also bind to some enzymes to form a dead-end complex before the binding of reduced flavin (38-40). To identify if 4-CP can bind to apoHadA, solutions of air saturated HadA (75 μM) that were pre-incubated with various concentrations of 4-CP (0.1–10 mM) were mixed with an anaerobic solution of $FADH^-$ (25 μM) to monitor the formation of C4a-hydroperoxy-FAD using a stopped-flow spectrophotometer. Final concentrations are given as after mixing. If a complex of HadA:4-CP can form, the reaction of enzyme-bound $FADH^-$ and oxygen would react differently from the reaction in the absence of 4-CP. Therefore, the kinetic traces of the reactions were measured at 380 (Fig. 8A) nm and 450 nm (Fig. 8B) to monitor whether or not the presence of 4-CP perturbs the formation of C4a-hydroperoxy-FAD. The results clearly show that upon increasing the 4-CP concentration, the amount of C4a-hydroperoxy-FAD formed decreased, and the kinetics of the reaction became more similar to that of the reaction of free $FADH^-$ with oxygen (not bound to HadA). At the highest 4-CP concentration used (orange line in Figs. 8A-B), the reaction was practically the same with the reaction of free $FADH^-$ reacting with oxygen (dashed line in Figs. 8A-B). These data clearly demonstrate that 4-CP can bind to HadA and this binding prevents the binding of $FADH^-$ to HadA i.e. 4-CP can bind to HadA to form a dead-end complex that cannot proceed through a productive path (Step 10 in Fig. 5). In another case in which HadA was pre-incubated with $FADH^-$ to form the HadA:$FADH^-$ binary complex prior to mixing with 4-CP (0.1–10 mM), it was found that at concentrations of 4-CP <2 mM, C4a-hydroperoxy-FAD can still form to the same extent as in the reaction in the absence of 4-CP (Fig. S9A). This implies that once the HadA:$FADH^-$ complex is formed, 4-CP cannot compete off the $FADH^-$ binding on HadA at concentrations <2 mM.

C.2. Formation of 4-CP and HadA leads to formation of a dead-end complex that does not result in dechlorination.

In order to confirm that formation of the HadA:4-CP complex (in section C.1) is not relevant to a productive path with dechlorination activity, the amounts of product (HQ) formed from two different mixing experiments in which HadA:4-CP was preformed, or not preformed (Figs. 8A-B and Fig. S9) were measured and compared. The results (*inset* in Fig. 8A) clearly show that higher amounts of 4-CP (>2 mM) reduced the amount of product formation in both mixing methods, indicating that 4-CP exerts a substrate inhibition effect. However, mixing of a preformed complex of HadA:4-CP plus oxygen with $FADH^-$ resulted in a much lower amount of product formation than the mixing of a binary complex of HadA:$FADH^-$ with oxygen plus 4-CP (*inset* in Fig. 8A). At 4-CP concentrations >3.2 mM, the preformed complex of HadA:4-CP did not give any dechlorinated product. This result also agrees with the kinetic traces because at this concentration of 4-CP, $FADH^-$ could not bind to HadA and only free $FADH^-$ oxidation was observed (orange line in Figs. 8A-B). All data suggest that 4-CP can bind to apoHadA to form a dead-end complex that does not lead to dechlorination (Step 10 in Fig. 5).

C.3 Binding kinetics and dissociation constant of the HadA:CP complex.

The rate of 4-CP binding to HadA was investigated using double-mixing stopped flow experiments. In the first mixing, an aerobic solution of HadA (75 μM) was mixed with 4-CP (0.8, 1.6, 3.2, and 6.4 mM) and was incubated at various time periods before the solution was mixed against an anaerobic solution of $FADH^-$ (25 μM) in the second mixing. Concentrations indicated are final concentrations. Longer incubation times and higher 4-CP concentrations allowed more complete formation of the HadA:4-CP complex, leading to the prevention of $FADH^-$ binding and the resulting free $FADH^-$ is oxidized with $t_{1/2}$ ~0.3 s. Therefore, the progress of 4-CP binding to HadA can be monitored by plotting ΔA450 nm at t=2 s *versus* incubation times of the first mixing. The plots were analyzed using an exponential equation to calculate the observed rate constant of HadA and 4-CP binding at each 4-CP concentration (Fig. S10A). The observed rate constant values were plotted against the 4-CP concentration to calculate k_{on}, k_{off} and K_d for the binding of 4-CP to HadA as 25 ± 2 $M^{-1}.s^{-1}$, 10 ± 2 × 10^{-4} s^{-1}, and 40 ± 10 μM, respectively (Fig. S10B).

A dissociation constant (K_d) for the binding of HadA and 4-CP could also be calculated from the amount of free $FADH^-$ in the system because the amount of free $FADH^-$ is inversely proportional to the amount of 4-CP occupying HadA. Analysis of the K_d value was carried out according to Equation S5 (*Supplemental Information*). Upon increasing the 4-CP concentration, more free $FADH^-$ oxidation which is oxidized faster than the HadA-bound $FADH^-$ (Fig. 8B) was observed. Therefore, the increase of absorbance at 450 nm at 2 s (which is due to free $FADH^-$ oxidation) with increasing 4-CP was used for calculating the K_d for the binding of HadA and 4-CP as 29 ± 4 μM (*inset* in Fig. 8B). This value agrees well with the dissociation constant obtained from the kinetics experiments mentioned above.

D. 4-CP binds to HadA after C4a-hydroperoxy-FAD is formed in the productive path. (Step 4 in Fig. 5).

The results in sections A-C indicate that $FADH^-$ is the first substrate to bind to HadA. Although 4-CP can bind to HadA, the HadA:4-CP is a dead-end complex that does not lead to formation of C4a-hydroperoxy-FAD. In order to proceed with the productive path, 4-CP must bind the HadA:$FADH^-$ complex or the HadA:C4a-hydroperoxy-FAD intermediate. To identify if 4-CP can bind to a binary complex of HadA:$FADH^-$ before it reacts with oxygen, two stopped-flow experiments were carried out to monitor rate constants of C4a-hydroperoxyFAD formation and decay. In the first experiment, a solution of HadA:$FADH^-$ in the presence of 4-CP was mixed with aerobic buffer while in the second experiment, a solution of HadA:$FADH^-$ binary complex alone was mixed with aerobic buffer plus 4-CP. Both experiments were monitored for absorbance changes at 380 and 450 nm to observe the formation of C4a-hydroperoxy-FAD. If the ternary complex can form, it likely reacts with oxygen differently from the reaction of the binary complex of HadA:$FADH^-$ with oxygen. Previous studies of C_2 oxygenase, which is also a two-component oxygenase, have shown that a ternary complex of C_2:$FMNH^-$:HPA reacts with oxygen ~50-fold

slower than the reaction of a binary complex of C_2:$FMNH^-$ (25). The results (Fig. S11) show similar kinetic traces for both experiments, indicating that pre-incubation of 4-CP with the HadA:$FADH^-$ binary complex had no influence on the rate constant of C4a-hydroperoxy-FAD formation. These results suggest that the a ternary complex of HadA:$FADH^-$:4:CP is not necessary and that 4-CP likely binds to the enzyme after C4a-hydroperoxy-FAD formation (Step 4 in Fig. 5).

E. Kinetics of HadA:$FADH^-$ binary complex reaction with O_2 in the presence 4-CP.

The results in Sections A-D have established the kinetic mechanism for the reaction of HadA from Steps 1-4 & 10 in Fig. 5. The knowledge obtained was used for setting up a mixing condition that allows the reaction of HadA to proceed in a productive manner by avoiding pre-mixing of HadA and 4-CP to prevent formation of the dead-end complex (Step 10 in Fig. 5) and by using HadA:$FADH^-$ with a ratio of 3:1 to allow for complete formation of an active HadA:$FADH^-$ binary complex.

E.1. Reaction of the HadA:$FADH^-$ binary complex with O_2 in the presence of 4-CP monitored by stopped-flow spectrophotometry.

A solution of HadA:$FADH^-$ (75 μM:25 μM) binary complex was mixed against buffer solutions containing 4-CP (0.8 mM) and various concentrations of oxygen (0.13, 0.31, and 0.61 mM) in 20 mM HEPES pH 7.5 at 25°C in the stopped-flow spectrophotometer. Concentrations indicated are given as final concentrations. Changes in absorbance at 380 and 450 nm were recorded to monitor the formation and decay of C4a-adduct intermediates and formation of the final species of oxidized FAD, respectively. The reaction in the presence of 4-CP (blue lines in Fig. 9) showed three observable phases. The first two phases are the same as those observed for the reaction performed in the absence of 4-CP (*upper inset* in Fig. 7), indicating that these two phases represent formation of C4a-hydroperoxy-FAD with a bimolecular rate constant of $7.0 \pm 0.2 \times 10^4$ $M^{-1}.s^{-1}$ and $3.8 \pm 0.3 \times 10^3$ $M^{-1}.s^{-1}$, respectively, as previously explained in Section B.1. The last phase showed a decrease of absorbance at 380 nm and a large increase of absorbance at 450 nm that is independent of oxygen concentration. The kinetics of this phase are significantly different from those data of the reaction in the absence of substrate. The rate constant of the reaction in the presence of 4-CP was $6.9 \pm 0.2 \times 10^{-2}$ s^{-1}, ~13 fold faster than that without substrate ($5.4 \pm 0.2 \times 10^{-3}$ s^{-1}). Although the kinetics showed only a single observable phase, this third phase is the combination of the reactions of a coupling path in which dechlorination (hydroxylation and Cl^- elimination) takes place (Steps 4-7 in Fig. 5) and an uncoupling path in which oxidized FAD is produced by H_2O_2 elimination (Steps 8&9 in Fig. 5). In order to obtain the individual rate constants associated with each reaction path, stopped-flow spectrofluorometric (Section E.2) and rapid-quench flow (Section E.3) experiments were carried out.

E.2. Detection of the hydroxylation rate constant by monitoring formation of the C4a-hydroxy-FAD intermediate using stopped-flow spectrofluorometry.

As the hydroxylation of 4-CP to form HQ requires the transfer of the hydroxyl group from C4a-hydroperoxy-FAD to the substrate to result in C4a-hydroxy-FAD, monitoring the kinetics of the change between the two forms of the flavin intermediates would be a direct measurement of the rate constant associated with hydroxyl group transfer from C4a-hydroperoxy-FAD into 4-CP. Previous studies have shown that C4a-hydroperoxyflavin and C4a-hydroxyflavin in some enzymes have different fluorescence characteristics (36,37,41-43), permitting direct measurement of the hydroxylation step. Therefore, an experiment similar to Section E.1 was carried out but the flavin fluorescence was monitored rather than absorbance. The fluorescence kinetics of the reactions in the presence of 4-CP was monitored by using excitation wavelengths at 380 nm (Ex380) and 450 nm (Ex450) to monitor emission of C4a-hydroxy-FAD and oxidized FAD, respectively. Both flavin species were detected by their fluorescence at emission wavelengths >495 nm (Em >495). The results showed three observable phases (red lines in Fig. 9). The first phase (0.001-0.2 s) is a lag phase with a very small change of fluorescence signal at both excitation wavelengths. This phase occurs at the same time as the formation of HadA:C4a hydroperoxy-FAD monitored by absorbance. These data indicate that HadA:C4a-hydroperoxy-FAD is not highly fluorescent. The

second phase (0.2-20 s) of the reaction showed a large increase in fluorescence at Ex380, but only a small change in fluorescence at Ex450. The observed rate constant of this phase was independent of oxygen concentration. This phase likely represents formation of C4a-hydroxy-FAD which is known to be more fluorescent than C4a-hydroperoxy-flavin (36,37,41-43). The last phase showed a large decrease in fluorescence at Ex380 and a large increase in fluorescence at Ex450, implying that this phase represents a dehydration reaction to eliminate H_2O from C4a-hydroxy-FAD to form oxidized FAD (Step 7 in Fig. 5). A control reaction in the absence of 4-CP was also carried out, and the result did not show any formation or decay of Ex380 species (Fig. S12); only the increase of fluorescence due to formation of oxidized FAD was observed. These results indicate that the fluorescence signal detected from Ex380 and Em >495 in the presence of 4-CP is indeed derived from C4a-hydroxy-FAD. Therefore, the rate constant of the formation of fluorescence species with Ex380 (second phase of the fluorescence trace, 0.36 ± 0.02 s^{-1}, $k_{obs,OH}$) represents the observed rate constant of the incorporation of –OH from C4a-hydroperoxy-FAD to 4-CP (the hydroxylation step, Step 5 in Fig. 5).

As the product yield for 4-CP hydroxylation is not 100%, the observed hydroxylation rate ($k_{obs,OH}$) is the combination of the rate constants from the coupling (Step 5 in Fig. 5) and uncoupling paths after 4-CP binding (Steps 9 in Fig. 5) and can be described according to the kinetic model for a bifurcation reaction (Eq. 1). The true hydroxylation rate constant (k_{OH} or k_5) that represents the hydroxylation step can be calculated based on the observed hydroxylation constant and product yield according to Eq. 2. The calculation yielded a hydroxylation rate constant for 4-CP (k_{OH} or k_5) of 0.18 ± 0.02 s^{-1}.).

$$k_{obs,OH} = k_{OH} + k_9 \qquad \text{Eq. 1}$$

$$\%yield\ product = \frac{k_{OH}}{k_{OH} + k_9} \qquad \text{Eq. 2}$$

E.3. Rate constant of product formation determined by rapid-quenched flow experiments.

Although the previous stopped-flow spectrofluorometric experiments could measure a rate constant associated with the hydroxylation step, the measurements were extrapolated only from observing changes in flavins (C4a-hydroperoxy-FAD, C4a-hydroxy-FAD and oxidized FAD) rather than from direct observation of the substrate 4-CP. Therefore, the rate constant associated with hydroxylation plus dechlorination of 4-CP was investigated using rapid-quench flow (RQF) techniques. The RQF experiment was carried out in the same manner as the stopped-flow experiments, except that only oxygen at a final concentration of 0.13 mM was used. The reactions were carried out in 20 mM HEPES pH 7.5 with 1 mM ascorbic acid at 25°C in the RQF machine that was placed inside an anaerobic glove box, and were quenched at various time points from 0-100 s by adding an equal volume of 0.2 M HCl (final concentration). Samples were collected, prepared, and analyzed by HPLC/DAD to measure the amount of HQ formation at various times (see *Experimental Procedures*) and the results are shown by the green circled line (Fig. 9).

The observed rate constant ($k_{obs,Pro}$) of product formation was calculated using a single exponential equation as 0.24 ± 0.01 s^{-1}. This value is in the same range as the observed rate constant of the hydroxylation step (Section E.2). As the reaction of HadA and 4-CP does not yield 100% product formation, the observed rate constant from RQF experiments ($k_{obs,Pro}$) also contain contributions from the uncoupling (H_2O_2 elimination) path similar to the explanation in E.2. Therefore, a rate constant associated with the product formation steps (k_{Pro}) was calculated by Eq. 3-4 as 0.12 ± 0.01 s^{-1}.

$$k_{obs,Pro} = k_{Pro} + k_9 \qquad \text{Eq. 3}$$

$$\%yield\ product = \frac{k_{Pro}}{k_{Pro} + k_9} \qquad \text{Eq. 4}$$

$$\frac{1}{k_{pro}} = \frac{1}{k_{OH}} + \frac{1}{k_{Eli}} \qquad \text{Eq. 5}$$

However, the rate constant of product formation is an observed value resulting from hydroxylation and chloride elimination reactions (Steps 5&6 in Fig. 5) which can be described according to the Eq. 5. As the hydroxylation rate constants (k_{OH}) can be calculated from measuring the kinetics of C4a-hydroxy-FAD formation (Section E.2), the rate constant associated with chloride elimination (k_{Eli} or k_6) was calculated as 0.36 ± 0.01 s^{-1} (Step 6 in Fig. 5).

F. Kinetics of the HadA:FADH$^-$ binary complex reaction with O_2 in the presence 4-CP at various pHs.

Reactions of HadA:FADH$^-$ and air saturated 4-CP were also carried out at various pHs from 6.5-10.5 to explore if the low product formation at pH <7.0 and >8.2 was due to the low yield of C4a-hydroperoxy-FAD in HadA (see *Experimental Procedures*). The kinetic traces obtained at absorbance 380 nm showed that at different pHs, the intermediates (C4a-hydroperoxy-FAD and C4a-hydroxy-FAD) form and decay at different rates (Fig. S13A). However, they all have highest absorbance values (combined signals from the two intermediates) in a similar range (within 10% variation). This is contrast to the yield of production formation at various pHs in which the yield variation is greater than 50% (Fig. 4). These data suggest that the variation of product formation at various pHs is not due to the impairment of HadA to form C4a-hydroperoxy-FAD but likely the protonation status of substrate or active site residues that can affect the hydroxylation process.

Overall reaction of HadA. The results from sections A-E have established the kinetic mechanism of the HadA reaction (Fig. 5). HadA binds FADH$^-$ as the first substrate to form a binary complex of HadA:FADH$^-$ that can be equilibrated in two forms in which both forms can react with oxygen to form HadA:C4a-hydroperoxy-FAD. 4-CP is the third substrate to bind to the enzyme after the reactive intermediate C4a-hydroperoxy-FAD is formed. The fate of the ternary complex of HadA:C4a-hydroperoxy-FAD:4-CP bifurcates into coupling (hydroxylation plus Cl^- elimination) and uncoupling paths of H_2O_2 elimination.

In the absence of 4-CP, the HadA:FADH$^-$ binary complex reacts with oxygen to form HadA:C4a-hydroperoxy-FAD in which it eliminates H_2O_2 slowly (0.005 s^{-1} at 25^{o}C). We propose that in the absence of 4-CP *in vivo*, the enzyme predominantly accumulates in the HadA:C4a-hydroperoxy-FAD form. This way, HadA can avoid formation of the HadA:4-CP dead-end complex and the enzyme is ready for dechlorination/hydroxylation activity. All kinetic and thermodynamic parameters of the individual steps are summarized in Table 2.

DISCUSSION

Our results reported herein are the first elucidation of the kinetic mechanism of a two-component flavin monooxygenase that can catalyze oxidative dechlorination of various CPs. These enzymes are prevalent in nature especially in microbes that have potential uses for CPs detoxification. Analysis of the products from single and multiple turnover reactions clearly demonstrate that HadA prefers to use 4-CP and 2-CP more than CPs with multiple substituents. Transient kinetics based on stopped-flow and rapid-quench flow experiments have shown the involvement of C4a-hydroperoxy-FAD and C4a-hydroxy-FAD in the oxidative dechlorination process of a two-component flavin-dependent dechlorinase. The data have also elucidated the order of substrate binding, the catalytic steps and the rate constants involved and have identified non-productive and productive paths of the HadA reactions.

Data from the single turnover reactions (Table 1) have clearly elucidated the substrate specificity of HadA. The experiments directly measured products resulting from the first catalytic cycle have shown that the hydroxylation efficiency of HadA with CPs are as follows: 4-CP ~ 2-CP > 2,4-DCP > 2,4,5-TCP > 2,4,6-TCP which is different from the previously published results of HadA investigation using the lysate of *E. coli* overexpressing the *hadA* gene which showed that the multi-substituted CPs were metabolized by the lysate more efficiently than mono-substituted CPs (14,15). It can be envisaged that for the lysate experiments, the overall bioconversion process can be influenced by other enzymes in the lysate that can further metabolize a first product. In single turnover experiments in which the purified HadA was used, the results can clearly state the substrate preference of HadA because other factors affecting the reaction efficiency such as the ability of a reductase to generate FADH$^-$ and efficiency of the FADH$^-$ transfer between the two proteins *versus* the loss of FADH$^-$ during turnover can be avoided. The results from single turnover reactions also agree well with the data from multiple turnover reactions in which purified HadA was reconstituted with C_1 reductase and G-6-PD. The data indicate that HadA prefers to use 4-CP > 2,4-DCP > 2,4,5-TCP > 2,4,6-TCP (Fig. 2 and Table 1).

Our results have expanded the understanding of the regio-selectivity of two-component flavin-dependent dechlorinases. Product analysis of 2,4,5-TCP bioconversion indicates that HadA prefers to initially catalyzes hydroxylation in conjunction with chloride elimination at position 4 and then later at position 2 (Fig. 3). HadA is specific to using $FADH^-$ as a substrate similar to TcpA and TftD (9-13). HadA has high sequence identity to TcpA from *R. eutropha* JMP134 (86.7%). Previously, analysis of TcpA substrate utilization was mainly done with 2,4,6-TCP and 2,4,6-TCP was specified as a native substrate for TcpA (11-13). Previous studies of TftD from *B. cepacia* AC1100 (64.2% identity to HadA) have compared substrate preference between 2,4,5-TCP and 2,4,6-TCP. The results indicate that TftD can utilize 2,4,5-TCP as a substrate faster than 2,4,6-TCP (9,10). Based on these previous and our results, it is likely that all three enzymes, HadA, TcpA, and TftD can use 2,4,5-TCP as a substrate more effectively than 2,4,6-TCP.

The ability of HadA to form C4a-hydroperoxy-FAD also demonstrates that the enzyme belongs to the Class D group of flavin-dependent monooxygenases (22) in which the enzymes form a C4a-hydroperoxyflavin intermediate that is necessary for the oxygenation reaction. This is similar to the other flavin-dependent monooxygenases such as C_2 from *A. baumannii* (25), luciferase from *Vibrio campbellii* (38), RebH from *Lechevalieria aerocolonigenes* ATCC 39243 (42), ActVA from *Streptomyces coelicolor* (44), Baeyer-Villiger monooxygenase (45), N-hydroxylating hydroxylases (46,47) *p*-hydroxybenzoate hydroxylase (48), and 3-hydroxybenzoate-6-hydroxylase (49). Previous investigations of TftD detected a species with a high absorption around the 390 nm region during multiple turnover reactions which was speculated to be a C4a-flavin adduct (9). With our current findings, it is very likely that the species previously detected in the multiple turnovers of TftD was either C4a-hydroperoxy-FAD or C4a-hydroxy-FAD. Studies of a single component pentachlorophenol hydroxylase (PcpB) from *S. chlorophenolicum* (18,19) also showed the existence of C4a-flavin adducts.

The transient kinetic studies in this report elucidated the order of substrate binding and identified the rate-limiting step in the overall reaction of HadA. For the productive path, HadA binds to $FADH^-$ as the first substrate to form a binary complex of HadA:$FADH^-$ that reacts with oxygen to result in C4a-hydroperoxy-FAD. The detection of highly fluorescent flavin species only after 4-CP binds to the C4a-hydroperoxy-FAD demonstrates the involvement of C4a-hydroxy-FAD in the HadA dechlorination. C4a-hydroxy-FAD has been shown to be highly fluorescent in flavin-dependent enzymes (36,37,41-43). As this step occurs before Cl^- elimination to form hydroquinone, the data suggest that the transfer of a terminal –OH from C4a-hydroperoxy-FAD to 4-CP to result in C4a-hydroxy-FAD occurs before Cl^- elimination. Based on the values of all the rate-constants involved in the reaction of HadA (Fig. 5 and Table 2), the hydroxylation step is a major rate-limiting step of the HadA reaction. This result agrees with computational calculation models of the reaction of TftD in which the hydroxylation step was proposed to be the rate-determining step for dechlorination (50). The involvement of C4a-flavin adduct species in the HadA reaction makes its mechanism unique from the mechanisms of reductive dehalogenation performed by tyrosine deiodinase from human (51,52) and glutathione-dependent dehalogenase from *S. chlorophenolicum* (53).

HadA also has various mechanistic properties distinct from other enzymes that make up the Class D monooxygenases. 4-CP can bind to HadA to form a dead-end complex of HadA:4-CP in which its binding obstructs the productive path of $FADH^-$ binding (Fig. 8). This result is different from those of the *p*-hydroxyphenylacetate hydroxylases (members of Class D monooxygenase) from *A. baumanii* and *Pseudomonas aeruginosa* in which the substrate HPA cannot bind to the apoenzymes (25,26,54). However, formation of an enzyme:substrate dead-end complex was also observed in bacterial luciferase (a member of the Class C monooxygenases) in which an aldehyde substrate can bind to the enzyme and prevent the binding of $FMNH^-$ that is required for proceeding to a productive path (39,40). However, as the rate constants of $FADH^-$ binding and formation of C4a-

hydroperoxy-FAD (Fig. 5 and Table 2) are much faster than the rate constant of H_2O_2 elimination, it is possible that under physiological conditions and in the absence of CPs, the enzyme mainly exists in the C4a-hydroperoxy-FAD form. This mode would be an efficient means for avoiding formation of a dead-end complex of HadA:4-CP such that the enzyme can be maintained in a state ready for the dechlorination process. When CPs are present, the ligand can bind to the HadA:C4a-hydroperoxy-FAD and the reaction can promptly proceed to a productive dechlorination path. C4a-hydroperoxyflavin is also thought to be a major species that accumulates during the reactions of *p*-hydroxyphenylacetate hydroxylase from *A. baumanii* and *Pseudomonas aeruginosa* under physiological conditions (25,26,54).

HadA can bind to $FADH^-$ and exist in two populations consisting of two different forms of HadA:$FADH^-$ that can react with oxygen to form C4a-hydroperoxy-FAD with different bimolecular rate constants. A longer incubation time resulted in more of the species that reacts slower with oxygen. This property does not exist in other enzymes in the Class D monooxygenases such as *p*-hydroxyphenylacetate hydroxylases (members of Class D monooxygenase) from *A. baumanii* and *Pseudomonas aeruginosa* (25,26,54). However, similar results have been observed in a few two-component monooxygenases in other classes. Similar properties were reported for a flavin-dependent halogenase or RebH (Class F monooxygenase). Preincubation of RebH and $FADH^-$ resulted in a less active form of RebH:$FADH^-$ that has a lower product yield (42). For alkanesulfonate monooxygenase or SsuD (Class C monooxygenase), when SsuD:$FADH^-$ was premixed prior to reacting with oxygenated substrate, the amount of product formation is 4-fold lower than that produced from the mixing of free $FMNH^-$ and a solution of SsuD containing oxygenated substrate (55). However, unlike in the HadA reaction, stopped-flow experiments of RebH and SsuD reactions in which complexes of enzyme and reduced flavins were preformed did not reveal formation of the C4a-hydroperoxyflavin intermediate (42,55). The results of the HadA reaction are similar to the stopped-flow results of luciferase from *Photobacterium leiognathi* TH1 (*Pl*LuxAB) in which two phases of C4a-hydroperoxy-FMN formation were detected when mixing a solution of preformed *Pl*LuxAB:$FMNH^-$ with O_2, while only one phase was detected in the non-premixed reaction (56). It is not clear why these enzymes possess this conformational change property. The mixture of enzyme populations that react differently with oxygen may be involved with the control of oxygen diffusion into the active site or the ability of reduced flavin to form the C4a-hydroperoxyflavin intermediate. It is known that diffusion of oxygen into a flavin-dependent monooxygenase can influence the rate of C4a-hydroperoxyflavin formation (57). Recently, it has been shown that formation of C4a-hydroperoxyflavin in a flavin-dependent enzyme occurs via a mechanism of proton-coupled electron transfer (58,59). In the C_2 reaction, in which the formation of C4a-hydroperoxyflavin is almost barrier-less with a bimolecular rate constant at 4^oC of 1.1×10^6 $M^{-1}s^{-1}$, a His residue that is located nearby the flavin C4a-position is necessary to facilitate the rapid formation of the intermediate (25,28). When we examined the X-ray structure of apoTcpA (PDB:4G5E) (21) that is similar to HadA and aligned it with the C_2 structure (PDB:2JBT) (60). His290 and Arg101 could be identified as potential proton donors at the active site. It is possible that the conformational change of HadA to a slower reacting species may be due to the change in the positions of these residues with respect to the flavin C4a-position, resulting in a slower rate of oxygen reaction. However, the conformational change in this case does not affect the overall turnover of HadA because the rate-limiting step of HadA is not the oxygen reaction step (Fig. 5 and Table 2).

Overall, the results in this report provide a solid basic mechanistic understanding of the flavin-dependent oxidative dechlorinases that will be useful for future applications. The data can also be used for comparison with future site-directed mutagenesis studies. As HadA homologs are found widespread in nature, an understanding of the HadA reaction (Fig. 5 and Table 2) also contributes to the general understanding of reactions of its homologs identified by SSN analysis (Fig. S1) (9,10,13,33-35). These enzymes were identified in microbes that showed potential in bioremediation applications.

In conclusion, this study is the first report of the kinetic mechanism of a flavin-dependent monooxygenase (dechlorinase) HadA from *R. pickettii* DTP0062. Combined approaches of transient kinetics have elucidated the order of substrate binding and rate constants associated with the individual steps. The data have also revealed the involvement of C4a-hydroperoxy-FAD and C4a-hydroxy-FAD in the oxidative dechlorination process. As the usage of CPs are still widespread world-wide, understanding how nature uses flavin and oxygen to battle these toxic chemicals provides knowledge that may lead to future innovations for detoxifying chemicals hazardous to human health.

EXPERIMENTAL PROCEDURES

Construction of the *hadA* gene. A synthetic gene of *hadA* based on the sequence GenBank: BAA13105 (15) was synthesized by GenScript (New Jersey, USA). The gene contains 1,554 nucleotides that encode for 517 amino acids. The *hadA* synthetic gene was digested with *NdeI* and *BamHI* restriction enzymes (Novagen) at the 5' and 3' ends, respectively before it was ligated with the *E. coli* expression vector, pET-11a to generate the *hadA*-pET-11a vector. The sequence of the *hadA*-pET-11a vector was analyzed (Macrogen) to verify its identity.

Protein expression. The *hadA*-pET-11a plasmid carrying a recombinant *hadA* gene was transformed into *E.coli* BL21 (DE3) cells. The resulting transformant was grown on an LB agar plate containing 50 µg/ml ampicillin at 37^{o}C overnight. Auto-induction medium (61) was used to grow cells and induce protein expression. Briefly, a single colony of grown cells was inoculated into 100 ml of ZYM-5052 starter medium containing 50 µg/ml ampicillin. The starter was incubated with shaking at 220 rpm, 37^{o}C overnight. Starting culture cells (1% of v/v) were then inoculated into six flasks of 650 ml ZYP-5052 broth containing 50 µg/ml ampicillin. The culture was incubated with shaking at 220 rpm, 37^{o}C until the OD_{600} reached 1.0. The temperature was then switched to 25^{o}C and the cultures were continuously shaken for an additional 16 hr. Cell paste was harvested by centrifugation and stored at -80^{o}C until needed.

Protein purification. The cell paste was suspended in 50 mM sodium phosphate (NaPi) pH 7.0 containing 5 mM ethylenediaminetetraacetic acid (EDTA), 100 µM phenylmethane sulfonyl fluoride (PMSF) and 1 mM dithiothreitol (DTT). Cells were disrupted by ultrasonication before being centrifuged at 27,000 g for one hour to discard cell debris. Ammonium sulfate ($(NH_4)_2SO_4$) precipitation (0-20%) was used to remove the remaining cell debris and other contaminant proteins. The protein fraction containing the HadA enzyme was precipitated in 20-40% $(NH_4)_2SO_4$. The resulting pellet was resuspended in ~50 ml of 30 mM NaPi pH 6.5 containing 50 mM NaCl (buffer A) and was dialyzed against 4 liters of buffer A. Denatured proteins were removed by centrifugation. The remaining clear solution of proteins was loaded onto a DEAE-sepharose^{TM} fast-flow (GE healthcare) anion exchange column (volume ~200 ml) which was pre-equilibrated with buffer A. The column was washed with 10 column volumes of buffer A to get rid of unbound proteins. Elution of protein was performed using a linear gradient of 50-400 mM NaCl in 30 mM NaPi pH 6.5. The fractions were pooled and concentrated, and the protein was exchanged into 20 mM HEPES pH 7.5 by passing it through a Sephadex^{TM} G-25 (GE healthcare) column. Purified protein was stored at -80^{o}C before use. All purification processes were performed at 4^{o}C. The total protein amount was determined using a Bradford assay and the purity of HadA was assessed by SDS-PAGE (15%) with coomassie brilliant blue staining and compared to standard protein markers (Enzmart Biotech, Thailand). Concentrations of purified HadA were determined based on absorbance 280 nm using the extinction coefficient value of 74.9 $mM^{-1}cm^{-1}$ calculated from ProtParam tool of ExPasy (http://web.expasy.org/protparam/).

Identification of products from single turnover reactions. A solution of HadA (75 µM) and FAD (25 µM) in 20 mM HEPES pH 7.5 was placed inside an anaerobic glove box to remove oxygen. The anaerobic solution of HadA:FAD was reduced by adding ~5 mg/ml dithionite stock solution into an equivalent amount (or slightly higher due to trace amount of oxygen) of FAD to produce HadA:$FADH^{-}$. Absorption spectra of the enzyme solution were monitored to ensure the complete reduction of the complex. The resulting mixture was mixed with an equal volume of air-saturated substrate (0.8 mM substrate and 0.13 mM oxygen)

in tightly closed microfuge tubes. Note that all reactions contained excess ascorbic acid (1 mM) in order to convert the resulting quinone product after Cl^- elimination into hydroquinone compounds that are more stable and easier to quantitate by HPLC analysis. All concentrations are indicated as final concentrations after mixing. The effect of ascorbic acid on the catalytic cycle of HadA was tested and it was found not to interfere with the HadA reaction. After mixing, the final concentrations of the reagents were half of the original concentrations. Under these conditions, $FADH^-$ was the limiting reagent and the reaction only proceeds for a single turnover. Reactions were left 15 minutes at room temperature before being quenched by adding an equal volume of acetonitrile. The resulting white precipitate of denatured protein was removed by centrifugation at 13,800 g, 4°C for 30 min. Supernatants were diluted three-fold in 20 mM HEPES pH 7.5 before being filtered through an Amicon® Ultra-0.5 centrifugal filter device with a molecular weight cutoff 10 kDa (Millipore). Filtrates were collected and analyzed by HPLC/diode array detector (DAD) or HPLC/DAD/mass spectroscopic detector (MSD) (Agilent) (see below). Commercially available substrates and products were purchased from Sigma-Aldrich, Merck, and Tokyo Chemical Industry Co., Ltd. (TCI). Standard curves of each authentic compound were constructed to calculate the amount of product formed or substrate consumed. Coupling percentage was calculated by comparing the product yield with the limiting reagent, $FADH^-$.

Bioconversion by multiple turnover reactions. Multiple turnover reactions of HadA were carried out by coupling the reaction with those of glucose-6-phosphate dehydrogenase (G-6-PD) (Sigma) and flavin reductase (C_1 from *A. baumannii*). Reactions (5 ml) contained substrate (100 μM), G-6-P (1 mM), G-6-PD (0.5 unit/ml), C_1 (1 μM), NAD^+ (5 μM), FAD (10 μM), HadA (10 μM) and ascorbic acid (1 mM) in 20 mM HEPES pH 7.5. Reactions were stopped at various time points to separate products from proteins similar to the protocol described above. The amount of product formed was analyzed using HPLC/DAD or HPLC/DAD/MSD as described below.

Product analysis. Products from single and multiple turnover reactions were analyzed using an HPLC (Agilent Technologies 1100 or 1260 Infinity series) equipped with a UV-visible diode array detector (DAD) and/or electrospray ionization mass spectroscopic detector (ESI-MSD) (Agilent Technologies 6120 Quadrupole LC/MS). The stationary phase was a Nova-Pak® (Waters) C18 reverse phase column with a 4 μm particle size and a 3.9 x 150 mm column size. Mobile phases were either a gradient of H_2O/methanol containing 0.1% formic acid or a gradient of H_2O/acetonitrile containing 0.1% formic acid. All HPLC grade solvents were purchased from Burdick & Jackson (B&J) scientific Co., Ltd. The HPLC was run at ambient temperature with a flow rate of 0.5 ml/min and a sample injection volume of 20 μl. The MSD was set in negative mode with a scan range of *m/z* from 10-500 or selected ion monitoring (SIM) mode that was set at the specific *m/z* of the substrate and expected product. Products were analyzed by comparing their HPLC retention time and mass with those of standard compounds.

pH effects on HadA reactions. In order to investigate the effects of pH on HadA, single turnover reactions of HadA using 4-CP as a substrate were carried out at various pHs. A pH jump method in which an enzyme solution in a lower ionic strength buffer at pH 7.5 was mixed with buffers with higher ionic strength at various pHs was employed. An anaerobic mixture of HadA and $FADH^-$ (75 μM and 25 μM, respectively) was prepared in 20 mM HEPES pH 7.5 as described above in an anaerobic glove box. To the mixture of HadA:$FADH^-$ was added an equal volume of air saturated 4-CP (0.8 mM and 0.13 mM oxygen) in a three buffer system consisting of *N*-(2-Acetamido)-2-aminoethanesulfonic acid (ACES):Tris:ethanolamine (ionic strength = 0.1 M) at various pHs with ascorbic acid (1 mM). This buffer system covered a pH range of 5.5-10.5 (62). Samples were processed and analyzed for product formation by HPLC/DAD as described above.

Transient kinetics of the HadA reaction. Single mixing or double-mixing stopped-flow spectrophotometers models SF-61SX and rapid-quench flow model RQF-63 from TgK Scientific (Bradford-on-Avon, UK) were used to monitor the kinetics of the HadA reaction. The flow path of the instrument was made anaerobic by flushing it with a solution of ~5 mg/ml sodium dithionite and leaving dithionite solution in the instrument

overnight before use. The flow unit was rinsed three times with anaerobic buffer that was bubbled with nitrogen gas to remove excess sodium dithionite before performing the experiment. To generate a solution of the HadA:$FADH^-$ complex, an anaerobic solution of FAD (25 μM) and HadA (75 μM) in 20 mM HEPES pH 7.5 was stoichiometrically reduced by adding an anaerobic solution of sodium dithionite (~5 mg/ml) in an anaerobic glove box. The reduced binary complex was placed inside an anaerobic glass tonometer and was later loaded onto the stopped-flow spectrophotometer. A solution of the HadA:$FADH^-$ complex was mixed with 20 mM HEPES pH 7.5 buffer containing 4-CP and various concentrations of oxygen at 25^{o}C in the stopped-flow instrument. Oxygenated buffers were prepared by bubbling the buffer with various mixtures of oxygen and nitrogen gases (final concentation of 0.13, 0.31, 0.61 mM oxygen) (25). Kinetic traces were obtained by monitoring the absorbance at wavelengths of 380 and 450 nm. Observed rate constants of the reactions were analyzed using ProgramA software (developed by Chiu C. J., Chang R., Diverno J., and Ballou D.P., at the University of Michigan, Ann Arbor, MI, USA). The rate constants of the oxygen dependent phases were plotted using KaleidaGraph software (Synergy Software) and analyzed as a bimolecular reaction with oxygen.

Analysis of Sequence Similarity Network (SSN).

A sequence similarity network (SSN) for HadA was carried out using the option A of Enzyme Function Initiative (EFI)-Enzyme Similarity Tool (EFI-EST, http://efi.igb.illinois.edu/efi-est/) and sequences from UniProt database that had identity to HadA of 34% or higher (63,64). SSN of HadA and its homologs were generated using an EFI alignment score of 70 (equivalent to grouping sequences of >27.74% in the same cluster). Networks of these sequences were visualized using Cytoscape version 3.2.1 (65).

ACKNOWLEDGEMENTS.

This research was financially supported by The Thailand Research Fund through grant RTA5980001, a grant from Mahidol University (to P.C.), and a Development and Promotion of Science and Technology Talents Project (DPST) Scholarship (to P. P.). We thank Ms. Paweena Choochuay and Ms. Philaiwarong Kamutira from Enzmart Biotech for helping with SDS-PAGE analysis of the purified HadA.

CONFLICT OF INETEREST.

The authors declare that they have no conflict of interest with the contents of this article.

AUTHOR CONTRIBUTION.

P.P. performed experiments, analyzed results and wrote manuscript. K.T. performed dechlorinase sequence analysis. J.S. gave suggestions on data analysis. P.C. conceived the study, analyzed results and wrote the manuscript.

REFERENCES

1. Danganan, C. E., Ye, R. W., Daubaras, D. L., Xun, L., and Chakrabarty, A. M. (1994) Nucleotide sequence and functional analysis of the genes encoding 2,4,5-trichlorophenoxyacetic acid oxygenase in *Pseudomonas cepacia* AC1100. *Appl. Environ. Microbiol.* **60**, 4100-4106
2. Dadson, O. A., Ellison, C. A., Singleton, S. T., Chi, L. H., McGarrigle, B. P., Lein, P. J., Farahat, F. M., Farahat, T., and Olson, J. R. (2013) Metabolism of profenofos to 4-bromo-2-chlorophenol, a specific and sensitive exposure biomarker. *Toxicology* **306**, 35-39
3. Agency for Toxic Substances and Disease Registry. (1999) Toxicological profile for chlorophenols. http://www.atsdr.cdc.gov/ToxProfiles/tp.asp?id=941&tid=195. (accessed December 1, 2016)
4. United States Environmental Protection Agency. (2014) Priority pollutant list. https://www.epa.gov/eg/toxic-and-priority-pollutants-under-clean-water-act#priority. (accessed December 1, 2016)
5. Agency for Toxic Substances and Disease Registry. (2015) Priority list of hazardous substances. http://www.atsdr.cdc.gov/spl/resources/ (accessed December 1, 2016).
6. Kovacic, P., and Somanathan, R. (2014) Nitroaromatic compounds: Environmental toxicity, carcinogenicity, mutagenicity, therapy and mechanism. *J. Appl. Toxicol.* **34**, 810-824
7. Olaniran, A. O., and Igbinosa, E. O. (2011) Chlorophenols and other related derivatives of environmental concern: properties, distribution and microbial degradation processes. *Chemosphere* **83**, 1297-1306
8. Igbinosa, E. O., Odjadjare, E. E., Chigor, V. N., Igbinosa, I. H., Emoghene, A. O., Ekhaise, F. O., Igiehon, N. O., and Idemudia, O. G. (2013) Toxicological profile of chlorophenols and their derivatives in the environment: the public health perspective. *Scientific World J.* **2013**, 1-11
9. Gisi, M. R., and Xun, L. (2003) Characterization of chlorophenol 4-monooxygenase (TftD) and NADH:flavin adenine dinucleotide oxidoreductase (TftC) of *Burkholderia cepacia* AC1100. *J. Bacteriol.* **185**, 2786-2792
10. Webb, B. N., Ballinger, J. W., Kim, E., Belchik, S. M., Lam, K. S., Youn, B., Nissen, M. S., Xun, L., and Kang, C. (2010) Characterization of chlorophenol 4-monooxygenase (TftD) and NADH:FAD oxidoreductase (TftC) of *Burkholderia cepacia* AC1100. *J. Biol. Chem.* **285**, 2014-2027
11. Louie, T. M., Webster, C. M., and Xun, L. (2002) Genetic and biochemical characterization of a 2,4,6-trichlorophenol degradation pathway in *Ralstonia eutropha* JMP134. *J. Bacteriol.* **184**, 3492-3500
12. Matus, V., Sanchez, M. A., Martinez, M., and Gonzalez, B. (2003) Efficient degradation of 2,4,6-Trichlorophenol requires a set of catabolic genes related to tcp genes from *Ralstonia eutropha* JMP134(pJP4). *Appl. Environ. Microbiol.* **69**, 7108-7115
13. Xun, L., and Webster, C. M. (2004) A monooxygenase catalyzes sequential dechlorinations of 2,4,6-trichlorophenol by oxidative and hydrolytic reactions. *J. Biol. Chem.* **279**, 6696-6700
14. Kiyohara, H., Hatta, T., Ogawa, Y., Kakuda, T., Yokoyama, H., and Takizawa, N. (1992) Isolation of *Pseudomonas pickettii* strains that degrade 2,4,6-trichlorophenol and their dechlorination of chlorophenols. *Appl. Environ. Microbiol.* **58**, 1276-1283
15. Takizawa, N., Yokoyama, H., Yanagihara, K., Hatta, T., and Kiyohara, H. (1995) A locus of *Pseudomonas Pickettii* DTP0602, *had*, that encodes 2,4,6-trichlorophenol-4-dechlorinase with hydroxylase-activity, and hydroxylation of various chlorophenols by the enzyme. *J. Ferment. Bioeng.* **80**, 318-326
16. Hatta, T., Fujii, E., and Takizawa, N. (2012) Analysis of two gene clusters involved in 2,4,6-trichlorophenol degradation by *Ralstonia pickettii* DTP0602. *Biosci., Biotechnol., Biochem.* **76**, 892-899

17. Xun, L., Topp, E., and Orser, C. S. (1992) Confirmation of oxidative dehalogenation of pentachlorophenol by a *Flavobacterium*. pentachlorophenol hydroxylase. *J. Bacteriol.* **174**, 5745-5747
18. Hlouchova, K., Rudolph, J., Pietari, J. M., Behlen, L. S., and Copley, S. D. (2012) Pentachlorophenol hydroxylase, a poorly functioning enzyme required for degradation of pentachlorophenol by *Sphingobium chlorophenolicum*. *Biochemistry* **51**, 3848-3860
19. Rudolph, J., Erbse, A. H., Behlen, L. S., and Copley, S. D. (2014) A radical intermediate in the conversion of pentachlorophenol to tetrachlorohydroquinone by *Sphingobium chlorophenolicum*. *Biochemistry* **53**, 6539-6549
20. Arora, P. K., and Bae, H. (2014) Bacterial degradation of chlorophenols and their derivatives. *Microb. Cell Fact.* **13**, 31-47
21. Hayes, R. P., Webb, B. N., Subramanian, A. K., Nissen, M., Popchock, A., Xun, L., and Kang, C. (2012) Structural and catalytic differences between two FADH(2)-dependent monooxygenases: 2,4,5-TCP 4-monooxygenase (TftD) from *Burkholderia cepacia* AC1100 and 2,4,6-TCP 4-monooxygenase (TcpA) from *Cupriavidus necator* JMP134. *Int. J. Mol. Sci.* **13**, 9769-9784
22. Huijbers, M. M., Montersino, S., Westphal, A. H., Tischler, D., and van Berkel, W. J. (2014) Flavin dependent monooxygenases. *Arch. Biochem. Biophys.* **544**, 2-17
23. Sucharitakul, J., Tinikul, R., and Chaiyen, P. (2014) Mechanisms of reduced flavin transfer in the two-component flavin-dependent monooxygenases. *Arch. Biochem. Biophys.* **555-556**, 33-46
24. Chaiyen, P., Suadee, C., and Wilairat, P. (2001) A novel two-protein component flavoprotein hydroxylase. *Eur. J. Biochem.* **268**, 5550-5561
25. Sucharitakul, J., Chaiyen, P., Entsch, B., and Ballou, D. P. (2006) Kinetic mechanisms of the oxygenase from a two-component enzyme, *p*-hydroxyphenylacetate 3-hydroxylase from *Acinetobacter baumannii*. *J. Biol. Chem.* **281**, 17044-17053
26. Sucharitakul, J., Phongsak, T., Entsch, B., Svasti, J., Chaiyen, P., and Ballou, D. P. (2007) Kinetics of a two-component *p*-hydroxyphenylacetate hydroxylase explain how reduced flavin is transferred from the reductase to the oxygenase. *Biochemistry* **46**, 8611-8623
27. Ruangchan, N., Tongsook, C., Sucharitakul, J., and Chaiyen, P. (2011) pH-dependent studies reveal an efficient hydroxylation mechanism of the oxygenase component of *p*-hydroxyphenylacetate 3-hydroxylase. *J. Biol. Chem.* **286**, 223-233
28. Thotsaporn, K., Chenprakhon, P., Sucharitakul, J., Mattevi, A., and Chaiyen, P. (2011) Stabilization of C4a-hydroperoxyflavin in a two-component flavin-dependent monooxygenase is achieved through interactions at flavin N5 and C4a atoms. *J. Biol. Chem.* **286**, 28170-28180
29. Tongsook, C., Sucharitakul, J., Thotsaporn, K., and Chaiyen, P. (2011) Interactions with the substrate phenolic group are essential for hydroxylation by the oxygenase component of *p*-hydroxyphenylacetate 3-hydroxylase. *J. Biol. Chem.* **286**, 44491-44502
30. Phongsak, T., Sucharitakul, J., Thotsaporn, K., Oonanant, W., Yuvaniyama, J., Svasti, J., Ballou, D. P., and Chaiyen, P. (2012) The C-terminal domain of 4-hydroxyphenylacetate 3-hydroxylase from *Acinetobacter baumannii* is an autoinhibitory domain. *J. Biol. Chem.* **287**, 26213-26222
31. Dhammaraj, T., Phintha, A., Pinthong, C., Medhanavyn, D., Tinikul, R., Chenprakhon, P., Sucharitakul, J., Vardhanabhuti, N., Jiarpinitnun, C., and Chaiyen, P. (2015) *p*-hydroxyphenylacetate 3-hydroxylase as a biocatalyst for the synthesis of trihydroxyphenolic acids. *ACS Catal.* **5**, 4492-4502
32. Dhammaraj, T., Pinthong, C., Visitsatthawong, S., Tongsook, C., Surawatanawong, P., and Chaiyen, P. (2016) A single-site mutation at Ser146 expands the reactivity of the oxygenase component of *p*-hydroxyphenylacetate 3-hydroxylase. *ACS Chem. Biol.* **11**, 2889-2896
33. Kitagawa, W., Kimura, N., and Kamagata, Y. (2004) A novel *p*-nitrophenol degradation gene cluster from a gram-positive bacterium, *Rhodococcus opacus* SAO101. *J. Bacteriol.* **186**, 4894-4902

34. Takeo, M., Yasukawa, T., Abe, Y., Niihara, S., Maeda, Y., and Negoro, S. (2003) Cloning and characterization of a 4-nitrophenol hydroxylase gene cluster from *Rhodococcus sp.* PN1. *J. Bios. Bioen.* **95**, 139-145
35. Takeo, M., Murakami, M., Niihara, S., Yamamoto, K., Nishimura, M., Kato, D., and Negoro, S. (2008) Mechanism of 4-nitrophenol oxidation in *Rhodococcus sp*. Strain PN1: characterization of the two-component 4-nitrophenol hydroxylase and regulation of its expression. *J. Bacteriol.* **190**, 7367-7374
36. Chaiyen, P., Brissette, P., Ballou, D. P., and Massey, V. (1997) Unusual mechanism of oxygen atom transfer and product rearrangement in the catalytic reaction of 2-methyl-3-hydroxypyridine-5-carboxylic acid oxygenase. *Biochemistry* **36**, 8060-8070
37. Luanloet, T., Sucharitakul, J., and Chaiyen, P. (2015) Selectivity of substrate binding and ionization of 2-methyl-3-hydroxypyridine-5-carboxylic acid oxygenase. *FEBS J* **282**, 3107-3125
38. Suadee, C., Nijvipakul, S., Svasti, J., Entsch, B., Ballou, D. P., and Chaiyen, P. (2007) Luciferase from *Vibrio campbellii* is more thermostable and binds reduced FMN better than its homologues. *J. Biochem.* **142**, 539-552
39. Francisco, W. A., Abu-Soud, H. M., Baldwin, T. O., and Raushel, F. M. (1993) Interaction of bacterial luciferase with aldehyde substrates and inhibitors. *J. Biol. Chem.* **268**, 24734-24741
40. Tinikul, R., and Chaiyen, P. (2016) Structure, Mechanism, and mutation of bacterial luciferase. *Adv. Biochem. Eng./Biotechnol.* **154**, 47-74
41. Maeda-Yorita, K., and Massey, V. (1993) On the reaction mechanism of phenol hydroxylase. New information obtained by correlation of fluorescence and absorbance stopped flow studies. *J. Biol. Chem.* **268**, 4134-4144
42. Yeh, E., Cole, L. J., Barr, E. W., Bollinger, J. M., Jr., Ballou, D. P., and Walsh, C. T. (2006) Flavin redox chemistry precedes substrate chlorination during the reaction of the flavin-dependent halogenase RebH. *Biochemistry* **45**, 7904-7912
43. Fagan, R. L., and Palfey, B. A. (2010) Flavin-dependent enzymes. in *Comprehensive Natural Products II: Chemistry and Biology*. pp 37-113
44. Valton, J., Mathevon, C., Fontecave, M., Niviere, V., and Ballou, D. P. (2008) Mechanism and regulation of the Two-component FMN-dependent monooxygenase ActVA-ActVB from *Streptomyces coelicolor*. *J. Biol. Chem.* **283**, 10287-10296
45. Orru, R., Dudek, H. M., Martinoli, C., Torres Pazmino, D. E., Royant, A., Weik, M., Fraaije, M. W., and Mattevi, A. (2011) Snapshots of enzymatic Baeyer-Villiger catalysis: oxygen activation and intermediate stabilization. *J. Biol. Chem.* **286**, 29284-29291
46. Mayfield, J. A., Frederick, R. E., Streit, B. R., Wencewicz, T. A., Ballou, D. P., and DuBois, J. L. (2010) Comprehensive spectroscopic, steady state, and transient kinetic studies of a representative siderophore-associated flavin monooxygenase. *J. Biol. Chem.* **285**, 30375-30388
47. Romero, E., Fedkenheuer, M., Chocklett, S. W., Qi, J., Oppenheimer, M., and Sobrado, P. (2012) Dual role of NADP(H) in the reaction of a flavin dependent N-hydroxylating monooxygenase. *Biochim. Biophy. Acta.* **1824**, 850-857
48. Palfey, B. A., and McDonald, C. A. (2010) Control of catalysis in flavin-dependent monooxygenases. *Arch. Biochem. Biophys.* **493**, 26-36
49. Sucharitakul, J., Tongsook, C., Pakotiprapha, D., van Berkel, W. J., and Chaiyen, P. (2013) The reaction kinetics of 3-hydroxybenzoate 6-hydroxylase from Rhodococcus jostii RHA1 provide an understanding of the *para*-hydroxylation enzyme catalytic cycle. *J. Biol. Chem.* **288**, 35210-35221
50. Li, Y. W., Zhang, R. M., Du, L. K., Zhang, Q. Z., and Wang, W. X. (2015) Insights into the catalytic mechanism of chlorophenol 4-monooxygenase: a quantum mechanics/molecular mechanics study. *RSC Adv.* **5**, 13871-13877
51. Bobyk, K. D., Ballou, D. P., and Rokita, S. E. (2015) Rapid kinetics of dehalogenation promoted by iodotyrosine deiodinase from human thyroid. *Biochemistry* **54**, 4487-4494

52. Hu, J., Chuenchor, W., and Rokita, S. E. (2015) A switch between one- and two-electron chemistry of the human flavoprotein iodotyrosine deiodinase is controlled by substrate. *J. Biol. Chem.* **290**, 590-600
53. Warner, J. R., and Copley, S. D. (2007) Pre-steady-state kinetic studies of the reductive dehalogenation catalyzed by tetrachlorohydroquinone dehalogenase. *Biochemistry* **46**, 13211-13222
54. Chakraborty, S., Ortiz-Maldonado, M., Entsch, B., and Ballou, D. P. (2010) Studies on the mechanism of *p*-hydroxyphenylacetate 3-hydroxylase from *Pseudomonas aeruginosa*: a system composed of a small flavin reductase and a large flavin-dependent oxygenase. *Biochemistry* **49**, 372-385
55. Zhan, X., Carpenter, R. A., and Ellis, H. R. (2008) Catalytic importance of the substrate binding order for the $FMNH_2$-dependent alkanesulfonate monooxygenase enzyme. *Biochemistry* **47**, 2221-2230
56. Tinikul, R., Pitsawong, W., Sucharitakul, J., Nijvipakul, S., Ballou, D. P., and Chaiyen, P. (2013) The transfer of reduced flavin mononucleotide from LuxG oxidoreductase to luciferase occurs via free diffusion. *Biochemistry* **52**, 6834-6843
57. Baron, R., Riley, C., Chenprakhon, P., Thotsaporn, K., Winter, R. T., Alfieri, A., Forneris, F., van Berkel, W. J., Chaiyen, P., Fraaije, M. W., Mattevi, A., and McCammon, J. A. (2009) Multiple pathways guide oxygen diffusion into flavoenzyme active sites. *Proc. Natl. Acad. Sci. U.S.A.* **106**, 10603-10608
58. Wongnate, T., Surawatanawong, P., Visitsatthawong, S., Sucharitakul, J., Scrutton, N. S., and Chaiyen, P. (2014) Proton-coupled electron transfer and adduct configuration are important for C4a-hydroperoxyflavin formation and stabilization in a flavoenzyme. *J. Am. Chem. Soc.* **136**, 241-253
59. Visitsatthawong, S., Chenprakhon, P., Chaiyen, P., and Surawatanawong, P. (2015) Mechanism of oxygen activation in a flavin-dependent monooxygenase: a nearly barrierless formation of C4a-hydroperoxyflavin via proton-coupled electron transfer. *J. Am. Chem. Soc.* **137**, 9363-9374
60. Alfieri, A., Fersini, F., Ruangchan, N., Prongjit, M., Chaiyen, P., and Mattevi, A. (2007) Structure of the monooxygenase component of a two-component flavoprotein monooxygenase. *Proc. Natl. Acad. Sci. U.S.A.* **104**, 1177-1182
61. Studier, F. W. (2005) Protein production by auto-induction in high density shaking cultures. *Protein Expr. Purif.* **41**, 207-234
62. Ellis, K. J., and Morrison, J. F. (1982) Buffers of constant ionic strength for studying pH-dependent processes. *Methods Enzymol.* **87**, 405-426
63. Atkinson, H. J., Morris, J. H., Ferrin, T. E., and Babbitt, P. C. (2009) Using sequence similarity networks for visualization of relationships across diverse protein superfamilies. *PloS One* **4**, e4345
64. Gerlt, J. A., Bouvier, J. T., Davidson, D. B., Imker, H. J., Sadkhin, B., Slater, D. R., and Whalen, K. L. (2015) Enzyme function initiative-enzyme similarity tool (EFI-EST): A web tool for generating protein sequence similarity networks. *Biochim. Biophys. Acta* **1854**, 1019-1037
65. Shannon, P. T., Grimes, M., Kutlu, B., Bot, J. J., and Galas, D. J. (2013) RCytoscape: tools for exploratory network analysis. *BMC Bioinformatics* **14**, 217-225

Table 1. Percentage of substrate dechlorination resulted from single and multiple turnover reactions

Substrate	Single turnover reaction		Multiple turnover reaction	
	Product*	**% Coupling**	**% Conversion**	**$t_{1/2}$ (min)**
4-CP	HQ	49 ± 4	100	13
2-CP	CHQ	43 ± 7[#]	-	-
2,4-DCP	CHQ	14 ± 1	100	35
2,4,5-TCP	2,5-DCHQ	9.0 ± 0.2	100	56
2,4,6-TCP	2,6-DCHQ	4.0 ± 0.3	72	nd

*Product was characterized in the presence of ascorbic acid. [#]Product formation from single turnover reactions were estimated based on the depletion of substrate. A dash (-) represents reactions that were not performed. (nd), $t_{1/2}$ of 2,4,6-TCP could not be analyzed because the reaction did not finish after 600 min.

Table 2. Summary of kinetic and thermodynamic parameters for the reaction of HadA:FADH$^-$ with 4-CP.

Step	Kinetic and thermodynamic* parameters	HadA:FADH$^-$ with 4-CP
1	k_1	$4.4 \pm 0.5 \times 10^3$ $M^{-1}.s^{-1}$
	$K_{D,FADH-}^*$	2.0 ± 0.2 µM
2	k_2	0.14 ± 0.01 s^{-1}
3	$k_{3.1}$	$7.0 \pm 0.2 \times 10^4$ $M^{-1}.s^{-1}$
	$k_{3.2}$	$3.8 \pm 0.3 \times 10^3$ $M^{-1}.s^{-1}$
5	k_5 or k_{OH}	0.18 ± 0.02 s^{-1}
6	k_6 or k_{Eli}	0.36 ± 0.01 s^{-1}
5+6	k_{Pro}	0.12 ± 0.01 s^{-1}
7	k_7	$6.9 \pm 0.2 \times 10^{-2}$ s^{-1}
8	k_8	$5.4 \pm 0.2 \times 10^{-3}$ s^{-1}
9	k_9	0.18 ± 0.03 s^{-1}
10	k_{10}	25 ± 2 M^{-1} s^{-1}
	k_{-10}	$10 \pm 2 \times 10^{-4}$ s^{-1}
	$K_{D,CP}^*$	40 ± 10 µM 29 ± 4 µM

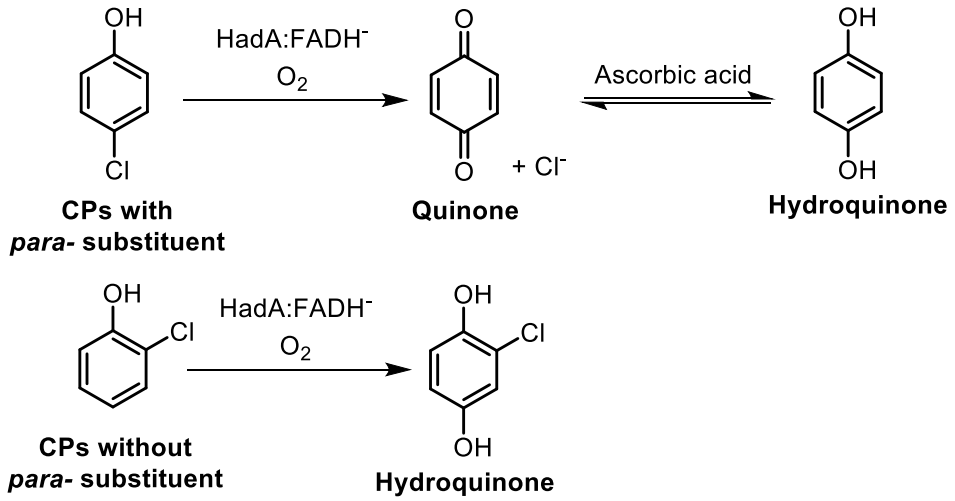

Figure 1. Reactions of HadA and chlorophenols with or without a *para-* substituent. For chlorophenols with a *para-* substituent, HadA catalyzes hydroxylation plus Cl^- elimination to yield quinone derivatives that can be reduced by ascorbic acid to form hydroquinone products (upper pathway). In the absence of a *para-* substituent, HadA catalyzes hydroxylation alone to yield hydroquinone (lower pathway).

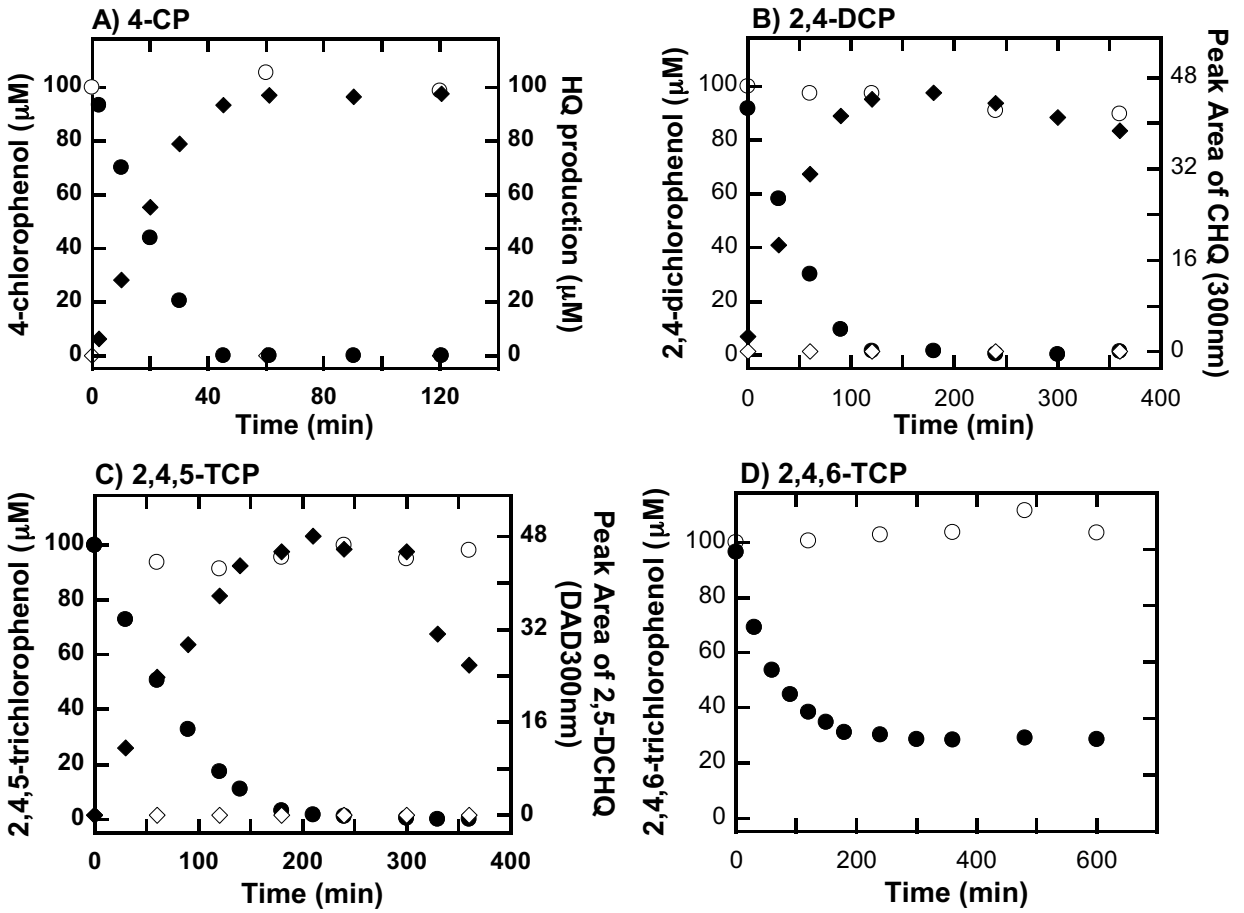

Figure 2. Multiple turnover reactions of HadA and chlorophenols. Plots of the amount of substrates remaining and product generated over time for reactions of *(A)* 4-CP, *(B)* 2,4-DCP, *(C)* 2,4,5-TCP and *(D)* 2,4,6-TCP are shown over a time course of 2-10 hr. Empty circles indicate substrate remaining in the control reaction without HadA. Filled circles indicate substrate remaining during multiple turnover reactions. Empty diamonds indicate product amount in the control reaction without HadA. Filled diamonds indicate product formed during multiple turnover reactions. For *(D)*, the amount of product from 2,4,6-TCP was unstable.

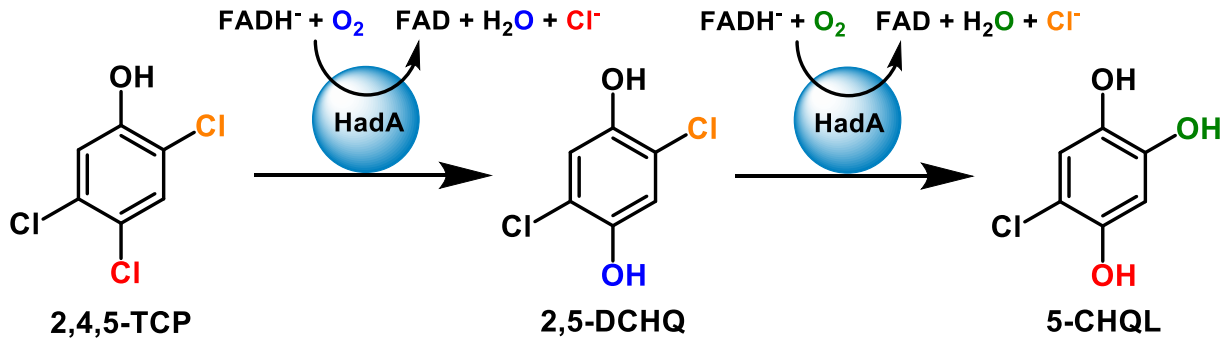

Figure 3. Catalytic reaction of HadA and 2,4,5-TCP. HadA initially catalyzes hydroxylation plus Cl^- elimination of 2,4,5-TCP at position 4, the first hydroxylation site, to generate 2,5-DCHQ as the first product. This step is followed by hydroxylation plus Cl^- elimination at position 2 to result in 5-CHQL.

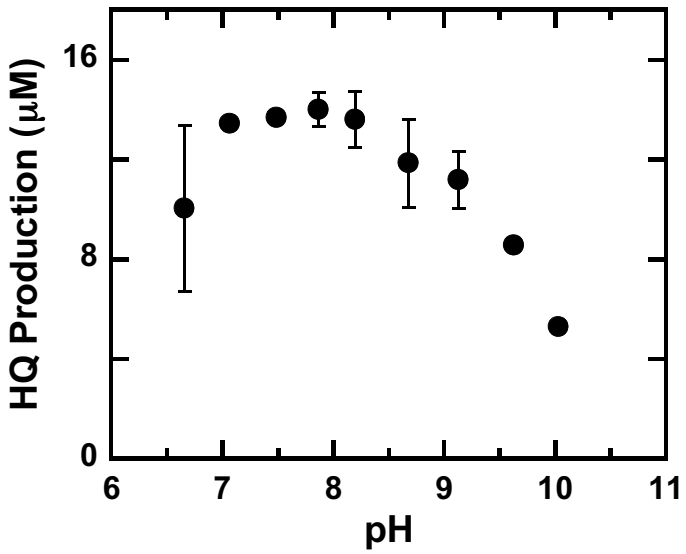

Figure 4. Optimum pH of the HadA catalytic reaction. Amount of product (HQ) generated from 4-CP from the single turnover reaction at various pH conditions (final pH of the reactions were 6.7, 7.1, 7.5, 7.9, 8.2, 8.7, 9.1, 9.6 and 10.0).

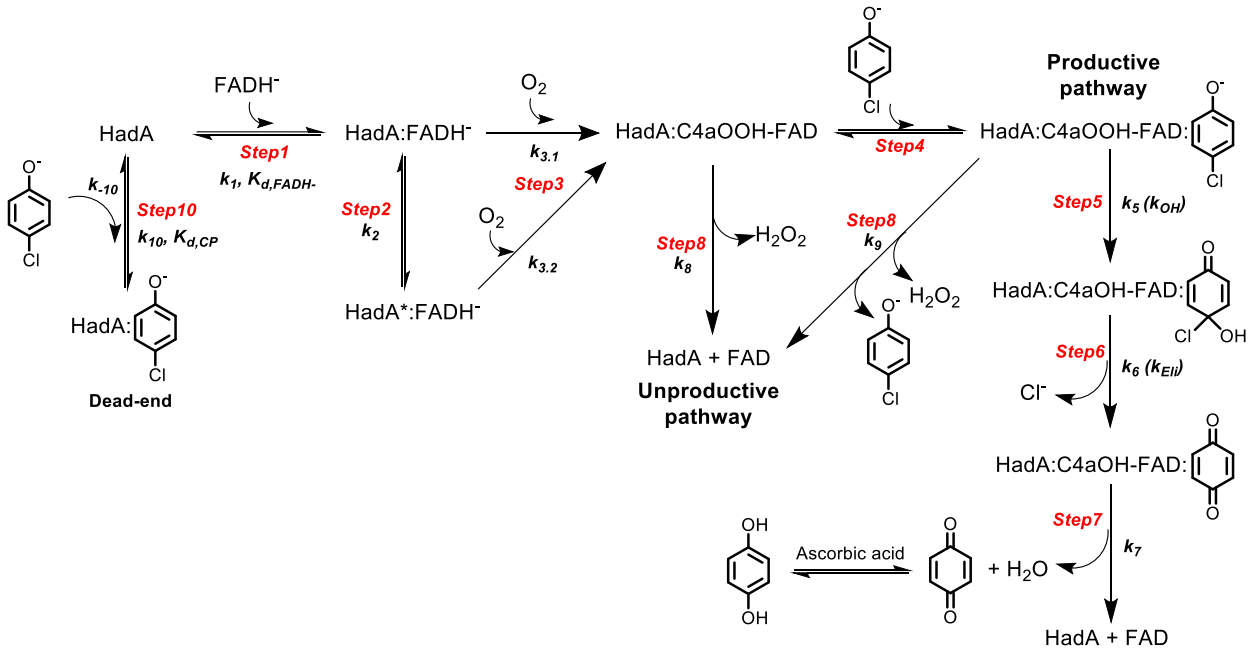

Figure 5. Kinetic mechanism of the HadA reaction with 4-chlorophenol. FAD is oxidized FAD, $FADH^-$ is reduced FAD, C4aOOH-FAD is C4a-hydroperoxy-FAD, and C4aOH-FAD is C4a-hydroxy-FAD.

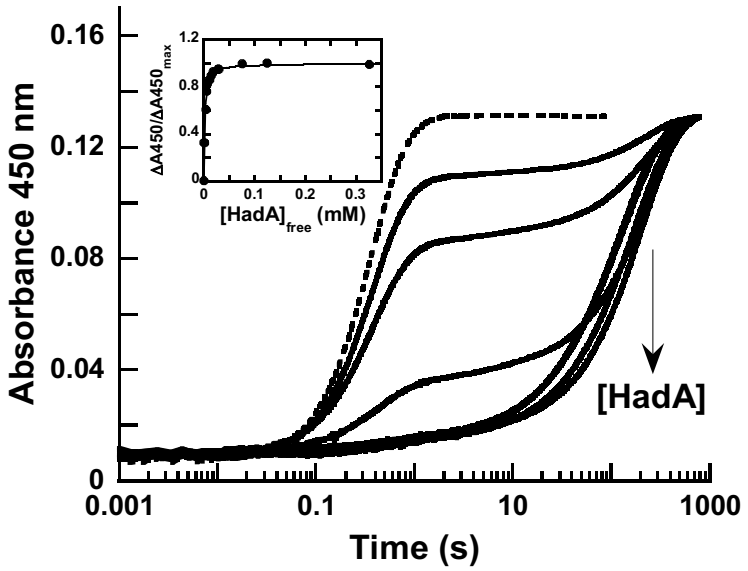

Figure 6. Kinetic traces for the binding of $FADH^-$ and HadA. Solutions of $FADH^-$ (12.5 μM) were mixed against various concentrations of HadA (0-0.4 mM) in 20 mM HEPES pH 7.5 at 25°C on the stopped-flow spectrophotometer. Results are shown in solid lines. For comparison, the re-oxidation of free $FADH^-$ is indicated by the dashed line. The *inset* shows a plot of the fraction of HadA:$FADH^-$ formation (ΔAbs450nm/ΔAbs450nm$_{max}$) *versus* the free HadA concentration.

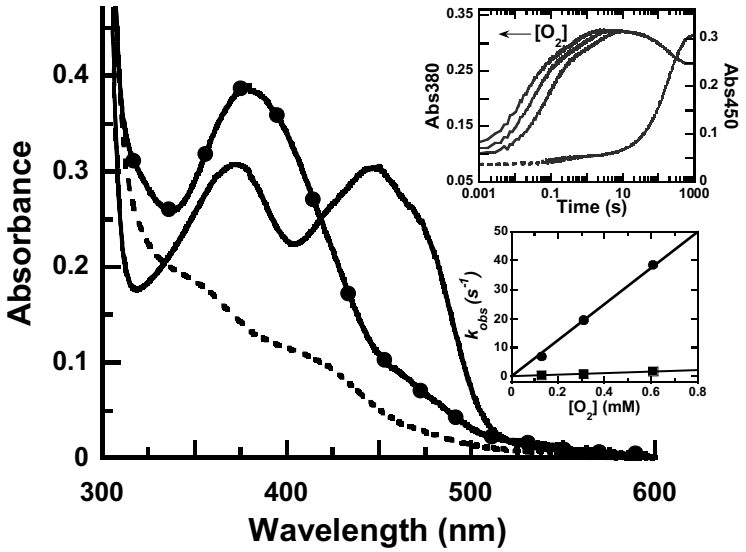

Figure 7. C4a-hydroperoxy-FAD in the reaction of HadA with oxygen. *Main Figure.* Spectra of the three flavin species involved in the catalytic cycle including the HadA:$FADH^-$ complex (dashed line), the HadA:C4a-hydroperoxy-FAD intermediate obtained at 10 s after the reaction started (solid line with filled circles) and a mixture of HadA and oxidized FAD (solid line). The *upper inset* shows kinetic traces of the reaction of the HadA:$FADH^-$ complex with oxygen monitored at 380 nm and 450 nm using stopped-flow spectrophotometry at 25°C, pH 7.5. The *lower inset* shows plots of the observed rate constants of the first phase (filled circle) and second phase (filled square) *versus* oxygen concentration.

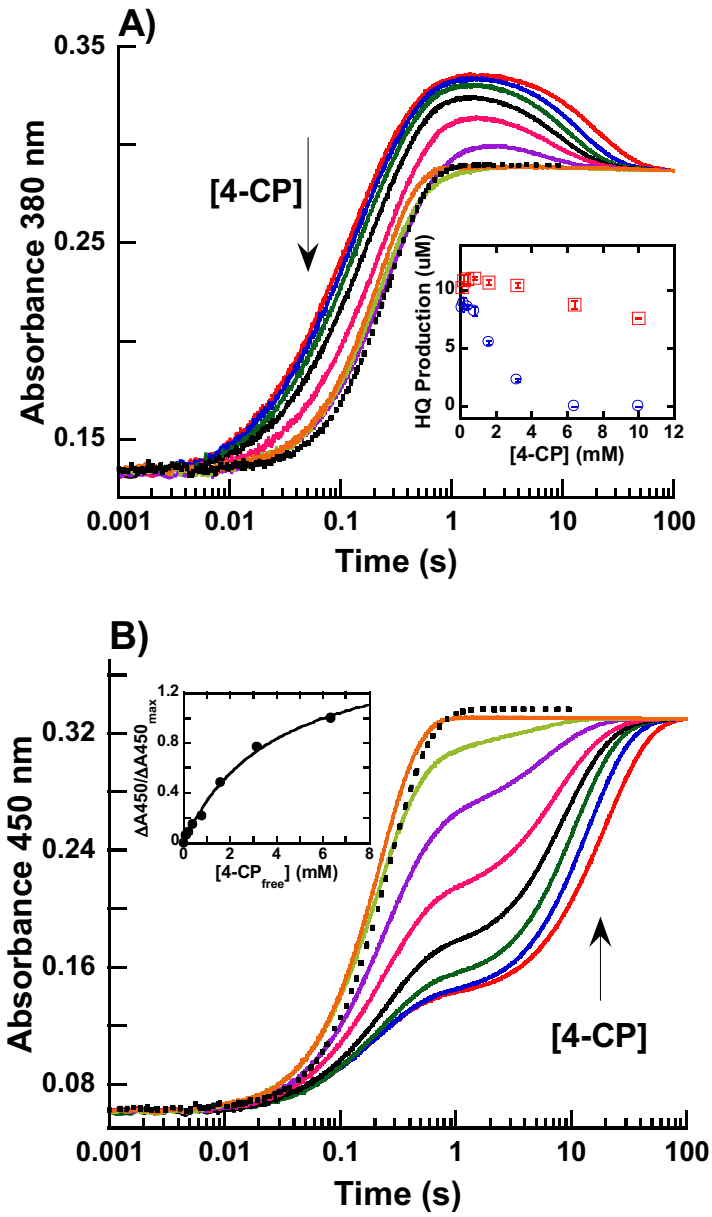

Figure 8. Reactions of a preformed HadA:4-CP complex with FADH$^-$. Kinetics of the reactions resulting from mixing a solution of air saturated HadA (75 µM) that was pre-incubated with various concentrations of 4-CP (0.1–10 mM) with an anaerobic solution of FADH$^-$ (25 µM) in the presence of 1 mM ascorbic acid in 20 mM HEPES pH 7.5. The reactions were monitored for absorption changes at the wavelengths 380 nm *(A)* and 450 nm *(B)*. Dashed lines in both figures represent reoxidation of FADH$^-$ in the absence of HadA. The *inset* in *(A)* is HQ product formation at various concentrations of 4-CP with two different mixing modes: mixing a solution of HadA:FADH$^-$ with an aerobic 4-CP (red square) *versus* mixing an aerobic solution of HadA:4-CP with an anaerobic solution of FADH$^-$ (blue circle). The *inset* in *(B)* is a plot between $\Delta A450nm/\Delta A450nm_{max}$ *versus* free 4-CP concentration.

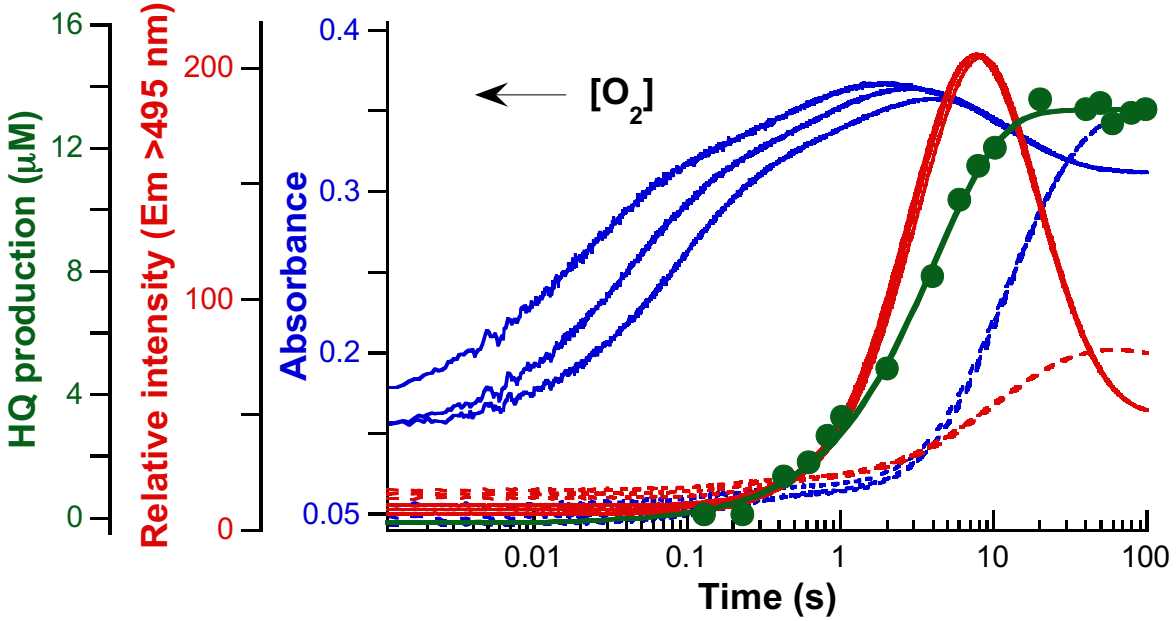

Figure 9. Kinetics of the reaction of HadA:FADH$^-$ with oxygen in the presence of 4-CP. Kinetic traces obtained from single turnover reactions of a HadA:FADH$^-$ binary complex (75 μM and 25 μM, respectively) with oxygenated 4-CP (0.8 mM 4-CP with 0.13, 0.31, and 0.61 mM oxygen) in 20 mM HEPES pH 7.5 at 25^{o}C. *Blue lines* are kinetic traces detected by stopped-flow spectrophotometry at wavelengths 380 (solid line) and 450 nm (dashed line). *Red lines* are fluorescence signal detected on a stopped-flow apparatus using the excitation wavelength of 380 nm (solid line) and 450 nm (dashed line) with emission wavelengths >495 nm. The *green line* is a calculated exponential curve that fits with HQ formation at each time point analyzed by rapid-quench flow (RQF) and HPLC/DAD techniques.